

AD-A055 944

FRANKLIN INST RESEARCH LABS PHILADELPHIA PA  
STRESS CORROSION ENVIRONMENTAL EFFECTS ON AF 1410.(U)  
1978 V V DAMIANO

F/G 11/6

UNCLASSIFIED

FIRL-03G-C4708-01

AFOSR-TR-78-1114

AFOSR-77-3341

NL

| OF |  
ADA  
065944

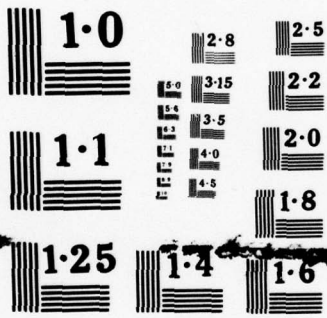


END

DATE  
FILMED

8 -78

DDC



NATIONAL BUREAU OF STANDARDS  
MICROCOPY RESOLUTION TEST CHART

AFOSR-TR- 78-1114

FOR FURTHER TRAN

2

AD A 055944

Technical

03G-C4708-01

Report

AD No. / DDC FILE COPY

Interim Report

STRESS CORROSION ENVIRONMENTAL EFFECTS ON AF 1410

GRANT NO.  
AFOSR-77-3341  
MOD NO 77-3341A

DDC  
JUN 30 1978  
F

Prepared for  
AFOSR - NA  
Bolling Air Force Base  
Washington, D.C. 20332

by  
Dr. Victor V. Damiano

Approved for public release;  
distribution unlimited.

 THE FRANKLIN INSTITUTE RESEARCH LABORATORIES  
THE BENJAMIN FRANKLIN PARKWAY • PHILADELPHIA, PENNSYLVANIA 19103

78 06 27 058

AIR FORCE OFFICE OF SCIENTIFIC RESEARCH (AFSC)  
NOTICE OF TRANSMITTAL TO DDC

This technical report has been reviewed and is  
approved for public release IAW AFR 190-23 (7b).  
Distribution is unlimited.

A. D. BLOSE  
Technical Information Officer

REPORT DOCUMENTATION PAGE		READ INSTRUCTIONS BEFORE COMPLETING FORM
1. REPORT NUMBER <b>AFOSR-TR- 78-1114<sup>v</sup></b>	2. GOVT ACCESSION NO.	3. RECIPIENT'S CATALOG NUMBER
4. TITLE (and Subtitle) STRESS CORROSION ENVIRONMENTAL EFFECTS ON AF 1410	5. TYPE OF REPORT & PERIOD COVERED INTERIM 1 May 1977 - 30 April 1978	
	6. PERFORMING ORG. REPORT NUMBER 03G-C4708-01 <sup>v</sup>	
7. AUTHOR(s) DR VICTOR V DAMIANO	8. CONTRACT OR GRANT NUMBER(s) AFOSR 77-3341 <sup>1av</sup>	
9. PERFORMING ORGANIZATION NAME AND ADDRESS THE FRANKLIN INSTITUTE RESEARCH LABORATORIES <sup>v</sup> 20th & PARKWAY PHILADELPHIA, PA 19103	10. PROGRAM ELEMENT, PROJECT, TASK AREA & WORK UNIT NUMBERS 2307B2 61102F	
11. CONTROLLING OFFICE NAME AND ADDRESS AIR FORCE OFFICE OF SCIENTIFIC RESEARCH/NA BLDG 410 BOLLING AIR FORCE BASE, D C 20332	12. REPORT DATE 1978	
	13. NUMBER OF PAGES 65	
14. MONITORING AGENCY NAME & ADDRESS (if different from Controlling Office)	15. SECURITY CLASS. (of this report)  UNCLASSIFIED	
	15a. DECLASSIFICATION/DOWNGRADING SCHEDULE	
16. DISTRIBUTION STATEMENT (of this Report)  Approved for public release; distribution unlimited.		
17. DISTRIBUTION STATEMENT (of this abstract entered in Block 20, if different from Report)		
18. SUPPLEMENTARY NOTES		
19. KEY WORDS (Continue on reverse side if necessary and identify by block number) STRESS CORROSION AF 1410 PLATES MECHANICAL PROPERTIES WELDED CRACK EXTENSION		
20. ABSTRACT (Continue on reverse side if necessary and identify by block number) AF 1410 plates available from Universal Cyclops through Air Force Materials Laboratory <del>under contract F33615-73-C-5093</del> were welded using filler wire fabricated from sheet stock of the same composition as the base plate. The method of welding was cold wire-gas tungsten arc using manual feed. Satisfactory welds having mechanical properties as welded approaching the properties of the base plate in the double austenitized and aged condition were obtained. Limited SCC tests demonstrate that nonhomogeneous microstructures in the fusion zone may result in nonuniform crack extension and seriously affect estimates made of KISCC.		

1978

(2)

Technical

(14) FIRL-03G-C4708-01

Report

*used*

(9) Interim Report. 1 May 77-30 Apr 78

(6) STRESS CORROSION ENVIRONMENTAL EFFECTS ON AF 1410.

GRANT NO.

(15) ✓ AFOSR-77-3341  
MOD NO 77-3341A

(16) 2307

(17) B2

(18) AFOSR

(19) TR-78-1114

DDC  
JUN 30 1978  
F

Prepared for

AFOSR - NA  
Bolling Air Force Base  
Washington, D.C. 20332

(10) by  
Dr. Victor V. Damiano

(11) 1978

(12) 68p.

142 925

THE FRANKLIN INSTITUTE RESEARCH LABORATORIES  
THE BENJAMIN FRANKLIN PARKWAY • PHILADELPHIA, PENNSYLVANIA 19103

78 06 27 058

## ABSTRACT

AF 1410 plates available from Universal Cyclops through Air Force Materials Laboratory under contract F33615-73-C-5093 were welded using filler wire fabricated from sheet stock of the same composition as the base plate. The method of welding was cold wire-gas tungsten arc using manual feed. Satisfactory welds having mechanical properties as welded approaching the properties of the base plate in the double austenitized and aged condition were obtained. Limited SCC tests demonstrate that nonhomogeneous microstructures in the fusion zone may result in nonuniform crack extension and seriously affect estimates made of  $K_{ISCC}$ .

ACCESSION for	
NTIS	White Section <input checked="" type="checkbox"/>
DDC	Buff Section <input type="checkbox"/>
UNANNOUNCED	<input type="checkbox"/>
JUSTIFICATION	
BY	
DISTRIBUTION/AVAILABILITY CODES	
Di.	SPECIAL
A	

## CONTENTS

<i>Section</i>	<i>Title</i>	<i>Page</i>
1	INTRODUCTION . . . . .	1-1
2	OBJECTIVES . . . . .	2-1
3	EXPERIMENTAL METHODS . . . . .	3-1
	3.1 Material . . . . .	3-1
	3.2 Welding Procedures . . . . .	3-2
	3.3 Stress Corrosion Cracking Tests . . . . .	3-5
	3.3.1 WOL Tests . . . . .	3-5
	3.3.2 Cantilever Beam SCC Tests . . . . .	3-7
	3.4 Scanning Electron Microscope Studies . . . . .	3-7
	3.5 Cinematography. . . . .	3-7
	3.6 Ultrasonics . . . . .	3-8
4	DISCUSSION AND RESULTS . . . . .	4-1
	4.1 Radiographic Tests . . . . .	4-1
	4.2 Mechanical Properties . . . . .	4-1
	4.3 WOL SCC Tests in 3.5% NaCl. . . . .	4-2
	4.4 Metallurgical and Chemical Homogeneity of Welds . . . . .	4-5
	4.5 Cantilever Beam SCC Tests . . . . .	4-7
5	FUTURE WORK . . . . .	5-1
6	SUMMARY . . . . .	6-1

ACKNOWLEDGEMENTS

REFERENCES

APPENDIX I FRACTURE MECHANICS APPROACH TO SCC

APPENDIX II RADIOGRAPHIC REPORTS ASME CODE

## FIGURES

<i>Number</i>	<i>Title</i>	<i>Page</i>
1	Metallographic Cross Sections of As-Received AF-1410 Sheet Showing the Oxide Layer (Top) and the Overall Cleanliness of the Steel. . . . .	3-9
2	Special Copper Back Up Plate Used to Purge Back Side of Weld . . . . .	3-11
3	Completed Weld Using AF-1410 Sheet Material as Filler Wire . . . . .	3-13
4	Joint Design AF-1410-2 and AF-1410-3. . . . .	3-15
5	Detailed Drawing of Modified WOL Specimen . . . . .	3-17
6(a)	WOL Samples from Weld and Base Plate AF-1410-2	
6(b)	WOL Sample from Weld AF-1410-3 . . . . .	3-19
7	NASA Clip Gage with Strain Gages in Place . . . . .	3-21
8	Calibration of Gage Opening vs. Gage Output . . . . .	3-23
9	Correlation of $K_1$ to $V_o$ . . . . .	3-25
10	NASA Clip Gage Arranged on WOL Specimen Ready for Application of Load by Torquing Bolt . . . . .	3-27
11	Cantilever Beam Test Ring for SCC Testing . . . . .	3-29
12	Cinematographic Apparatus Showing Dual 16mm Cameras WOL Specimen and Corrosion Cell for the Continuous Monitoring of Crack Propagation . . . . .	3-31
13	WOL Specimens with Transducer for Ultrasonic Evaluation of Crack Growth and the Krautkraner System . . . . .	3-33
14(a)	Fracture Surface of AF-14-10-2 Weld Tested by MetCut	
14(b)	Fracture Surface of AF-1410-2 Weld Tested by FIRL	
14(c)	Fracture Surface of AF-1410 Base Plate Tested by FIRL . . . . .	

## FIGURES

<i>Number</i>	<i>Title</i>	<i>Page</i>
14(a)	Fracture Surface of AF 1410-2 Weld Tested by MetCut	
(b)	Fracture Surface of AF 1410-2 Weld Tested by FIRL	
(c)	Fracture Surface of AF 1410 Base Plate Tested by FIRL . . . . .	4-15
14(d)	Enlarged View of Figure 14(b) Showing Irregular Fatigue Crack Front	
(e)	Enlarged View of Figure 14(c) Showing Fatigue Crack and Sec Crack . . . . .	4-17
15	Crack Propagation in AF-1410-2 Weld and Base Plate $K_{10} = 40 \text{ ksi } \sqrt{\text{in}}$ . . . . .	4-19
16	Crack Extension vs. Time <u>WOL</u> Test of AF-1410 Base Plate $K_{10} = 40 \text{ ksi } \sqrt{\text{in}}$ . . . . .	4-21
17	Weld Cross Sections with Hardness Impressions . . . . .	4-23
18	Back Scattered Electron Image of Weld AF-1410-2 at Positions 1 and 2 in Table V . . . . .	4-25
19	Back Scattered Electron Image of Weld AF-1410-2 at Positions 3 and 4 Shown in Table V . . . . .	4-27
20	Back Scattered Electron Image of Weld AF-1410-2 at Positions 5 and 8 Shown in Table V . . . . .	4-29
21	Back Scattered Electron Images of Weld AF-1410-3 at Positions 1 and 2 Shown in Table VI . . . . .	4-31
22	Back Scattered Electron Images of Weld AF-1410-3 at Positions 3 and 4 shown in Table VI . . . . .	4-33
23	Back Scattered Electron Images of Weld AF-1410-3 at Positions 5 and 6 Shown in Table VI . . . . .	4-35
24	Fusion Zone Mechanical Properties from Little & Machmeirer . . . . .	4-37

## 1. INTRODUCTION

Most high strength steels have characteristically low fracture toughness and low resistance to stress corrosion cracking. Through a cooperated effort by United States Steel (USS) and the Naval Ship Research Development Laboratory under NAVSHIPS Contract NObs-88540 and 94535 a 10Ni-2Cr-1Mo-8Co-.11C Steel (Hy-180) was developed which provided the best compromise of high strength, toughness, excellent stress corrosion cracking resistance and weldability. Extensive stress corrosion cracking evaluation of a family of Hy-180/210 candidate alloys led to the selection of an optimum alloy composition in which  $K_{1\text{ SCC}}$  values of both the plates and weld metal were in the range of 130 to 150 ksi  $\sqrt{\text{in}}$ . Minor alterations in the composition and purity resulted in a higher degree of susceptibility of the alloy to SCC. Air melted base metal and gas tungsten arc (GTA) welded 12N-5Cr-3Mo steel systems resulted in  $K_{1\text{ SCC}}$  values of 44 to 33 ksi  $\sqrt{\text{in}}$  for the base plate and weld respectively.

Hy-180 although having a high strength and high fracture toughness was not competitive on a weight to strength basis with other candidate material for aircraft structural application. A new alloy AF1410 (14Co-10Ni-2Cr-1Mo-0.16C) was developed jointly by General Dynamics and U.S. Steel by sponsorship of the Air Force Materials Laboratory under contract F33615-73-C-5093. The mechanical property goals set in this program was ultimate tensile strength (UTS) of 230/280 k, tensile yield (TY) of 220 ksi and plane strain fracture toughness  $K_{1c} \geq 115$  ksi  $\sqrt{\text{in}}$ . Details of the rational and experimental work associated with the development and evaluation of AF1410 are summarized in AFML-TR-75-148.

Pilot plant production quantities of 2000 pound heats were produced exhibiting the desired mechanical properties. Only a limited number of stress corrosion cracking tests were conducted on the baseplate. Values of  $K_{1\text{ SCC}} > 100$  ksi were reported but the results were questionable due to crack branching and deviation from ASTM 399-70.

The potential for large scale usage of AF 1410 as a structural aircraft material demonstrated in the AFML-TR-75-148 project, led to the development of commercial practices for the manufacture of production quantities of AF 1410 by Universal Cyclops Specialty Steel Div. under AFML contract F33615-76-C-5026.

Recent data reported by Universal Cyclops on the mechanical properties of their production quantities indicates that the goal of UTS = 230/250. TYS = 220 ksi and  $K_{Ic} = 120 \text{ ksi } \sqrt{\text{in}}$  had been achieved. Stress corrosion cracking testing of this material is presently being conducted by Universal Cyclops.

The weldability of AF-1410 by cold wire-gas tungsten arc (CW-GTA), hot wire gas tungsten arc (HW-GTA) and electron beam weld processes was also investigated under AFML Contract F33613-73-C-5013 and reported in AFML-TR-75-148. All welding in these studies were performed with automatic welding equipment. The filler metal composition used for CW-GTA and HW-GTA in accordance with studies made on 10Ni-Cr-Mo-Co by (USS) was close in the major alloying elements to AF-1410 base plate with the exception to residual elements aluminum, silicon and vanadium. These elements were increased above the level of the base plate to achieve an optimum deoxidation effect. The sulfur, oxygen, and nitrogen were held to low levels in the weld wire and in the deposited weld. Carbon was held to  $\sim 0.1\%$ . The welding parameters for the CW-GTA processes for optimum properties included low energy input and low deposition rates. The manual CW-GTA process was not investigated although manual processes are conducive to low energy input and low deposition rates. The mechanical properties achieved by the automatic CW-GTA process did meet the minimum strength requirements after post aging heat treatment. No  $K_{ISCC}$  testing to evaluate the stress corrosion cracking sensitivity of welds was conducted.

Recent data obtained by Rockwell International indicates that values of  $K_{ISCC}$  for Universal Cyclops prepared AF-1410 base plate of  $30 \text{ ksi } \sqrt{\text{in}}$  in 3.5% NaCl solution are typical for the double austenitized and aged condition (950 °F - 5 hrs.). Welds made with weld wire prepared by U.S. Welding in Tarzana, California gave values of  $K_{ISCC} = 60 \text{ ksi } \sqrt{\text{in}}$ .

C4708-01

The present research program supported by AFOSR under contract 77-3341 is concerned with the study of stress corrosion cracking of welded AF 1410 in both aqueous and gaseous environments using material supplied by AFML through Universal Cyclops. The grant issued May 1, 1977 is under the direction of Dr. Victor V. Damiano who is the principal investigator. The following interim report covers the period May 1, 1977 to April 30, 1978.

## 2. OBJECTIVES

The objective of the program is to investigate the sensitivity of welded AF 1410 plates to stress corrosion cracking in both aqueous and gaseous environments and to study the nature of subcritical growth crack in welds including crack growth rates, crack path and the interrelation of these factors to the solidification inhomogeneities arising in the welds.

The specific goals of the program included:

1. The preparation of welds using a manual cold wire - tungsten arc technique (CW-GTA) and commercially available AF-1410 and weld wire of the same composites as the base plate.
2. The evaluation of the quality of the welds using radiographic analysis, scanning electron microscopy and mechanical tests.
3. The evaluation of the stress corrosion cracking sensitivity of the welds using plane strain conditions and a fracture mechanics approach in both aqueous and gaseous environment.
4. The study of the subcritical crack growth rates and path using cinematographic recording of in situ crack propagation.
5. The correlation of subcritical crack growth behavior to the solidification structures produced by welding.

The final results of this program may have practical significance with respect to the feasibility of field weld repairs of AF-1410 aircraft structures.

## 3. EXPERIMENTAL METHODS

## 3.1 MATERIAL

AF-1410 plates were furnished by Universal Cyclops with permission of the Air Force Officer under contract F33615-76-C-5026. Twenty plates of 4" x 8" x 5/8" and twenty plates of 4" x 8" x 1" were received in the double austenitized condition (1650 °F/30 min/WQ + 1500 °F/30 min/W.Q.) from heat #L3550K19. Details of the melting and fabrication of this heat are given in Report IR-160-6 (I), (II), and (III).

The mechanical properties reported for this heat after aging at 950 °F 5 hrs./AC and processing to 1.25" plate are given in Table I.

Table I.

<u>Heat</u>	<u>Test Direct</u>	<u>UTS ksi</u>	<u>Yield Strength</u>	<u>Elong. %</u>	<u>Red. in Area</u>	<u>CVN R.T Ft. lbs.</u>	<u>Hardness R<sub>c</sub></u>
L3550K19	L	246.5	226.6	17.2	72.9	71.5	48.1
	L	248.8	231.2	15.6	71.5	68.0	
	T	255.9	234.2	15.2	68.5	61.0	48.2
	T	254.2	233.8	15.9	71.2	69.0	

The composition of this heat stirred ingot is given below.

<u>C</u>	<u>Mn</u>	<u>Si</u>	<u>S</u>	<u>P</u>	<u>CR</u>	<u>Ni</u>	<u>Co</u>	<u>Mo</u>	<u>Al</u>	<u>Ti</u>	<u>N</u>	<u>O</u>	<u>Fe</u>
0.17	0.06	0.03	0.002	0.004	2.05	10.19	14.01	1.04	0.001	0.004	0.001	0.0002	Bal.

Preliminary studies in welding were conducted using 1/16" wide strips cut from 0.062 thick sheet stock also supplied by Universal Cyclops from heat #3616 K13.

The surface of the sheets, which had a mill scale were cleaned by mechanical abrasion of the surface. Metallographic samples were prepared from each sheet to determine the extend of the oxide penetration and to evaluate the overall cleanliness of the material. The micrographs shown in Figures 1A and B reveal the surface oxide scale and a fine oxide dispersion.

The sheets were sheared into strips approximately 1/16" wide and 13" long. These strips were used as the feed wire in the welding of plates AF 1410-1, AF 1410-2, and AF 1410-3 described in section 3.2.

Weld wire (0.062) dia of the same composition as the base plate also prepared by Universal Cyclops was received later in the program and all additional welding was conducted using this weld wire.

Weld wire having an adjusted composition in the residual elements Al, Si and vanadium was not available so that all the welds were prepared using weld wire of the same composition as the base plate.

### 3.2 WELDING PROCEDURES

Procedures for GTA welding of 10Ni-Cr-Mo-Co steel were described in Technical Report, Project No. 33018-007(51) by The Applied Research Laboratory (USS) and for 14Co-10Ni-1Mo-0.1C (AF 1410) by General Dynamics Report ERR-FW-1565.

In these studies, an attempt was made to maintain the residuals (Mn, Si, Al, V, and Ti) to minimum levels and S, P, O, and N at very low levels. Both of the above references indicate that additions of 0.10 to 0.20% Si and up to 0.02% Al and 0.10% V was required in the weld wire composition to prevent porosity in the welds and to achieve optimum toughness.

In the present work, no attempt was made to adjust the level of the residuals of the weld wire. Commercially available sheet stock having the same composition as the base plate from heat L3616-K13 was used in the preliminary welding experiments as shown in Table II. 0.062 dia. weld wire prepared from heat L3616-K14 presently being used for welding is also shown in Table II.

Table II

<u>Heat</u>	<u>C</u>	<u>Mn</u>	<u>Si</u>	<u>S</u>	<u>P</u>	<u>Cr</u>	<u>Ni</u>	<u>Co</u>	<u>Mo</u>	<u>Al</u>	<u>Ti</u>
L3616-K13	0.16	0.13	0.03	0.002	0.005	2.07	10.00	13.95	0.95	0.002	0.004
L3616-K14	0.16	0.09	0.04	0.001	0.003	0.94	10.00	13.98	0.96	0.003	0.005
		<u>N</u>	<u>O</u>	<u>Fe</u>							
		0.007	0.0011	Bal							
		0.0004	0.0015	Bal.							

Since acceptable weld parameters were established in the prior studies for the CW-GTA process, and the process lends itself to manual feed, it was selected as the method of welding for the present studies. The CW-GTA process although being very slow and inefficient is well suited for the present study since high quality welds can be prepared with a minimum tendency to pick up residuals such as oxygen, nitrogen and hydrogen and the process has practical application in the field for weld repair.

The welding was performed using a 300 amp Linde UCC 305 machine, with foot attachment for amperage control in conjunction with a Linde HW-20 water cooled torch. A contact pyrometer was used to monitor the interpass temperature.

A preliminary test weld was run utilizing the 5/8" thick plates and the joint design shown in Table III. This plate was designed as AF-1410-1.

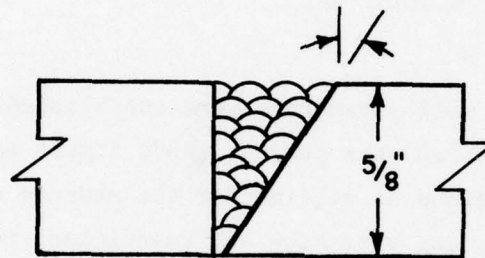
A Special back-up fixture shown in Figure 2 was used for all manual CW-GTA welds to provide auxiliary back-up gas shielding. The completed weld is shown in Figure 3.

The welding parameters used are given in Table III. Two additional weld joints were made using the 1" thick plates after it was determined that AF-1410-1 was satisfactory. These plates designated AF-1410-2 and AF-1410-3 were welded along the 8" edge of the plates. The joint design for these plates is shown in Figure 4. The double V design was selected for the SCC test since it presented a more symmetrical design for crack propagation studies parallel to the weld beads.

Table III

PRELIMINARY  
JOINT DESIGN

AF1410-1 Test Weld

Welding Parameters

Amps - Root Pass 120-130, Filler Passes 130-140

Volts - 12-13

Travel Speed - Avg. 2.75 IPM

Tungsten - 3/32 Dia. 2% thoriated

Wire - .080" sheet sheared into strips .080" wide

Torch gas - Argon @ 15 CFh

Back up gas - Argon @ 5 CFh

Preheat Temp - None

Interpass Temp. - 200°F Max.

Energy Input - 31.2 KJ

The included angle for AF-1410-2 was 90° while that for AF-1410-3 was 60°. The included angle was decreased in plate 3 to shorten the welding time and reduce the amount of filler metal required for the weld.

Plate AF-1410-4 was also prepared with the double V joint design similar to AF-1410-3. Filler wire used to weld AF-1410-4 was 0.062" dia. wire supplied by Universal Cyclops.

All welds were analyzed with X-ray radiography by Magnaflux Corporation and rated according to ASME code. Welds were cross sectioned and metallographic, electron probe studies and hardness measurements were made.

Charpy V notch and tensile tests were made of the fusion zone.

### 3.3 STRESS CORROSION CRACKING TESTS

#### 3.3.1 WOL Tests

Plates measuring 8" x 4" x 1" which were welded along the 8" edge provided 2 WOL - 1 x T specimens for stress corrosion cracking tests. The samples were machined and fatigue cracked by Met Cut Research Associates following Novak and Rolfe's [2] modified WOL specimen design as shown in Figure 5.

WOL samples machined from AF 1410-2 and AF-1410-3 are shown in Figure 6(a) and (b) respectively. Figure 6(a) shows one base plate WOL sample and one weld WOL sample. The second weld WOL sample was evaluated for  $K_{1\text{ SCC}}$  by Met Cut Research Associates.

Figure 6(b) shows the position of two weld WOL samples. The extra piece shown was used for mechanical test evaluation.

the NASA displacement gage shown in Figure 7 was constructed according to ASTM Designation E399-70T, Appendix A1 following details given by Fisher, Bubsez and Srawley [3].

The gage consists of two cantilever beams and a spacer block which are clamped together with a single nut and bolt as shown in Figure 7.

The material used for the gage was 13V-11Cr-3Al titanium alloy in the solution treated condition because of its high yield strength to modulus ratio. Four 120  $\Omega$  strain gages were mounted longitudinally on each side of the beams as close as possible to the beam-spacer block. The gage bonding conformed to the manufacturer's specification.

The gage was calibrated using a calibrated eyepiece of a light microscope - Figure 8(b). The mv output/volt input vs. displacement of the gage are plotted in Figure 8(a). The gage was linear over the range of 0.200 to 0.250".

Nominal crack opening displacement  $V_o$  required to initially load 1-T modified WOL specimens of AF 1410 to a given P or  $K_{10}$  value are plotted in Figure 9. These data were generated from the relationship

$$V_o = \frac{K_{10}}{E} \times \frac{a_o B}{B}^{1/2} \frac{C_6}{C_3}$$

where E is the modulus

$A_o$  is the original crack length

$B_n$  is the specimen thickness

$B = 1"$

$C_6$  and  $C_3$  are a function of  $\frac{a}{W}$

as given in Appendix 1.

The NASA clip gage was inserted into the clips of the WOL specimen. The sample was gripped in a vise and the bolt, after lubrication, was torqued to provide the desired  $K_{10}$  as determined from the graph, Figure 8. The arrangement of the NASA clip gage on the specimen ready for application of load is shown in Figure 10.

WOL specimens are loaded to a given  $K_{10}$  above the suspected  $K_{1 SCC}$  value immersed in the environment of test and crack movement is monitored on a continuous basis.

### 3.3.2 Cantilever Beam SCC Tests

4" x 8" x 1" plates welded along the 4" length will provide four test specimens measuring approximately 1" x 1" x 16" for cantilever beam SCC tests as developed by Brown. [4] The pre-notched and fatigue cracked bar is held horizontally and surrounded at the notch by the corrodant. The specimen is dead-weight loaded for periods of time extending to a minimum of 500 hours under various loading conditions. The apparatus following Brown's design is shown in Figure 11. The stress intensity factor  $K_{\alpha}$  is calculated for various loading conditions as described in Appendix I.

The cantilever beam SCC tests is better suited than the WOL specimen to measure differences in the SCC sensitivity parallel and perpendicular to the weld bead. By incorporating a step loading procedure it is possible to minimize the number of samples required for establishment of a  $K_{1SCC}$  value.

### 3.4 SCANNING ELECTRON MICROSCOPE STUDIES

The JSM-50A scanning electron microscope (SEM) equipped with energy dispersive x-ray capability (EDXA) and a Northern Scientific 880 computer-based system was used to analyze the metallurgical and chemical homogeneity of the welds. For chemical analysis ZAF (atomic number-absorption-fluorescence) correction routines were used for matrix corrections.

Back scatter electron imaging was used to document the structures observed at the locations where chemical data were obtained.

### 3.5 CINEMATOGRAPHY

The apparatus for the continuous monitoring of crack path and crack growth rates utilizing cinematography is shown in Figure 12. The loaded WOL sample is placed in the corrosion cell and either single frame or short bursts of 6 to 10 frames may be taken on a continuous basis without interruption of the test. Either aqueous or gaseous environments can be studied with this apparatus. Crack growth rates and crack paths will be documented on 16 mm film.

### 3.6 ULTRASONICS

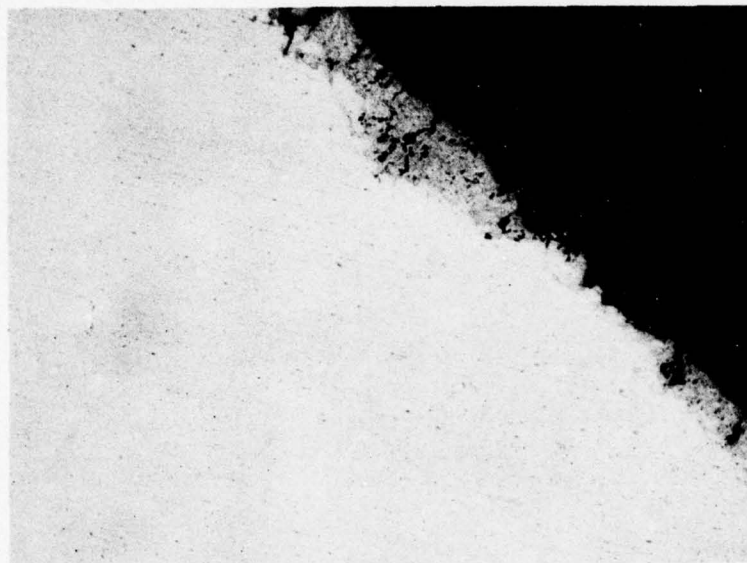
Monitoring of crack extensions in fracture toughness tests was demonstrated by Klems, Fisher and Buzzard [5]. The method has also been used successfully for monitoring fatigue crack growth. It has not been used for stress corrosion cracking monitoring. In the present study the single transducer pulse-echo technique utilizing longitudinal waves will be investigated to determine whether crack movement at the center of the WOL specimen can be monitored in a SCC test. The transducer specimen arrangement and the Krautkramer system is shown in Figure 13. Glycerine is used as a coupling agent for transmitting ultrasonic energy. The transducer is clamped on the top of the specimen and positioned so that reflection of the waves at the tip of the fatigue crack is observed as a spike on the cathode ray tube. As the crack propagates, the reflected energy from the crack tip increases and the output voltage at the observed spike increases. The reflected signal may be time gated and continuously monitored with a recorder. The rate of increase in the reflected signal from the crack tip then may be used to estimate the crack growth at the center of the specimen. It is not known at this time how the presence of corrodant in the crack will affect the output signal. The technique may be best suited for SCC studies in gaseous environments.

The feasibility of using ultrasonics to measure crack growth rates in stress corrosion cracking tests is not known but will be evaluated in the next period of this program.

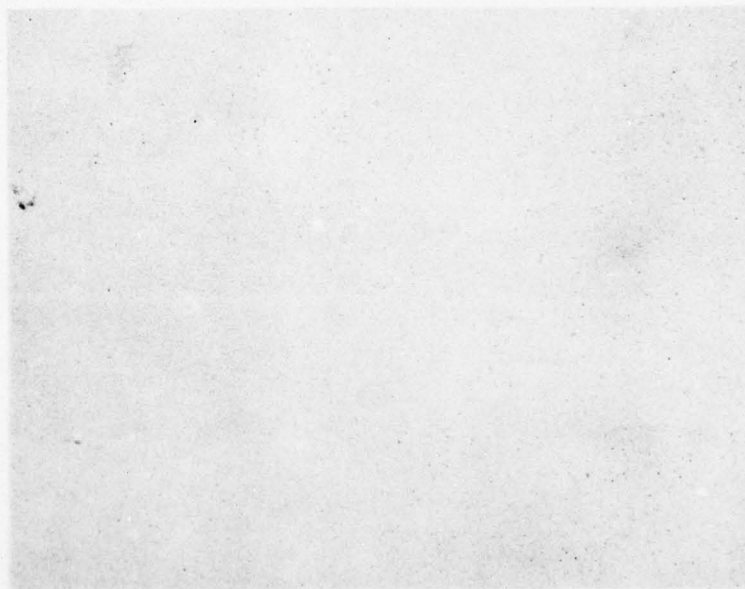
After completion of the stress corrosion test all samples will be fractured and the crack front will be measured at the surfaces and the interior of the specimen.

The nature of the fracture and the three dimensional aspects of the crack path will also be investigated.

C4708-01



A



B

**Figure 1. Metallographic Cross Sections of As-Received AF 1410 Sheet Showing the Oxide Layer (Top) and the Overall Cleanliness of the Steel.**

- A) - Surface Scale
- B) - Internal Cross Section Mag. 150X

C4708-01

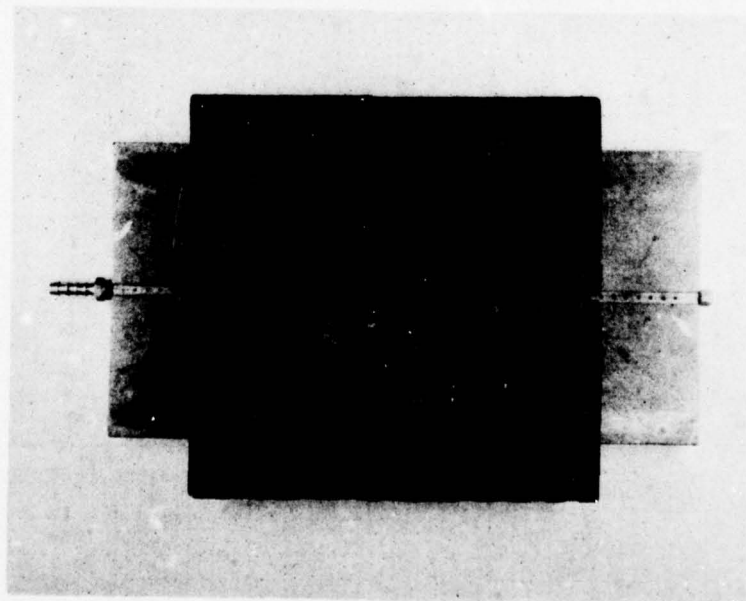
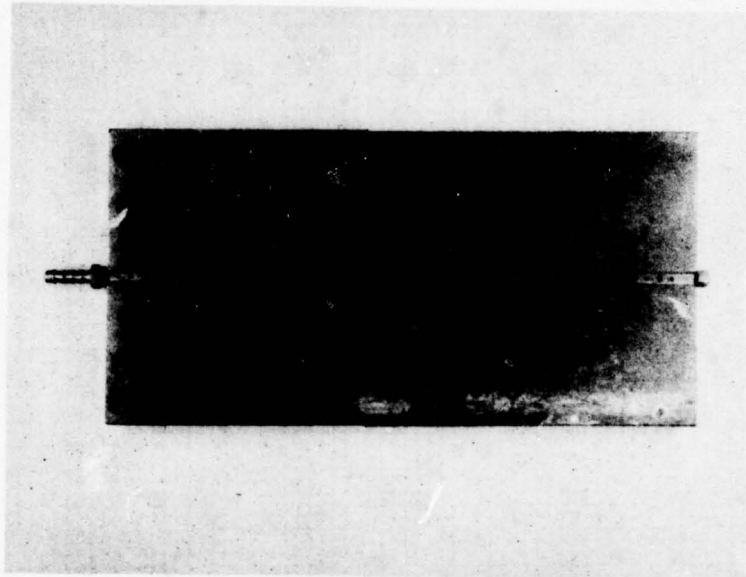


Figure 2. Special Copper Back Up Plate Used to Purge Back Side of Weld



Top of Weld A



Bottom of Weld B

Figure 3. Completed Weld Using AF 1410 Sheet Material as Filler Wire

PRECEDING PAGE BLANK-NOT FILMED

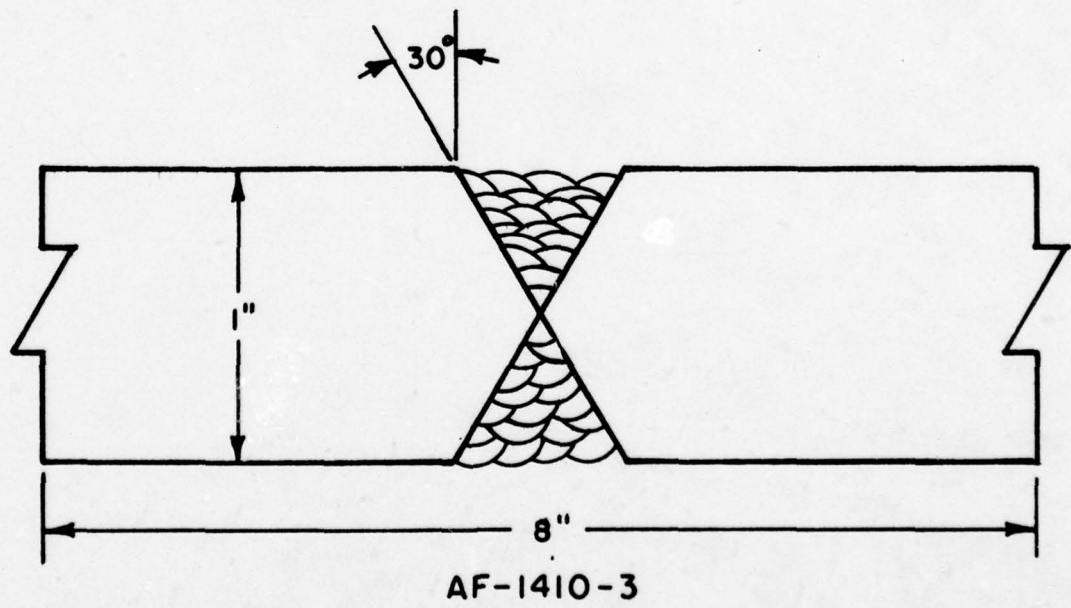
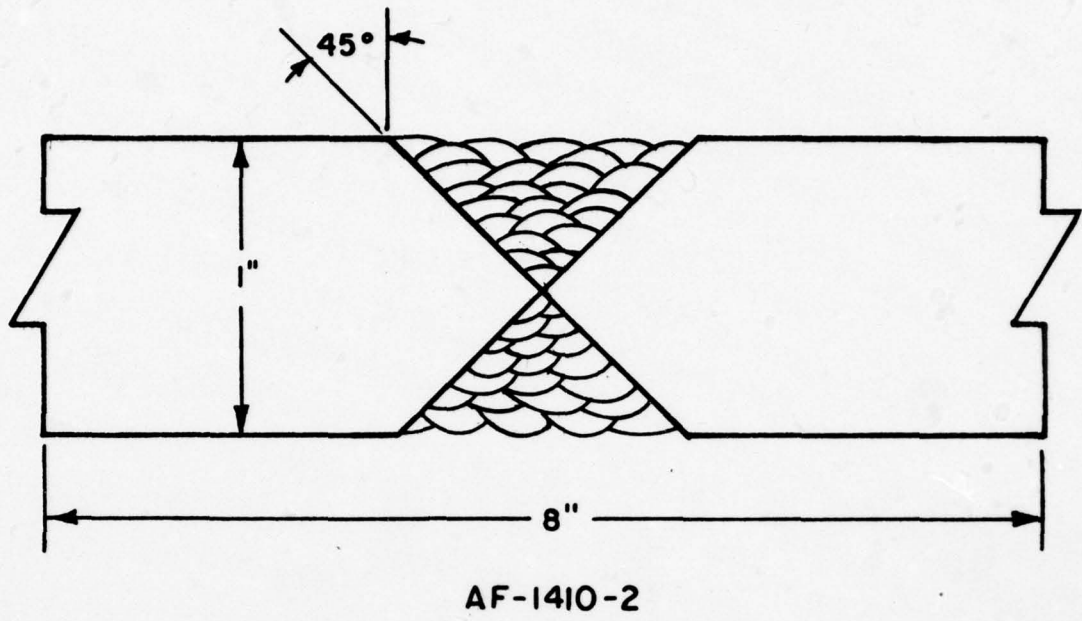


Figure 4. Joint Design AF-1410-2 and AF-1410-3

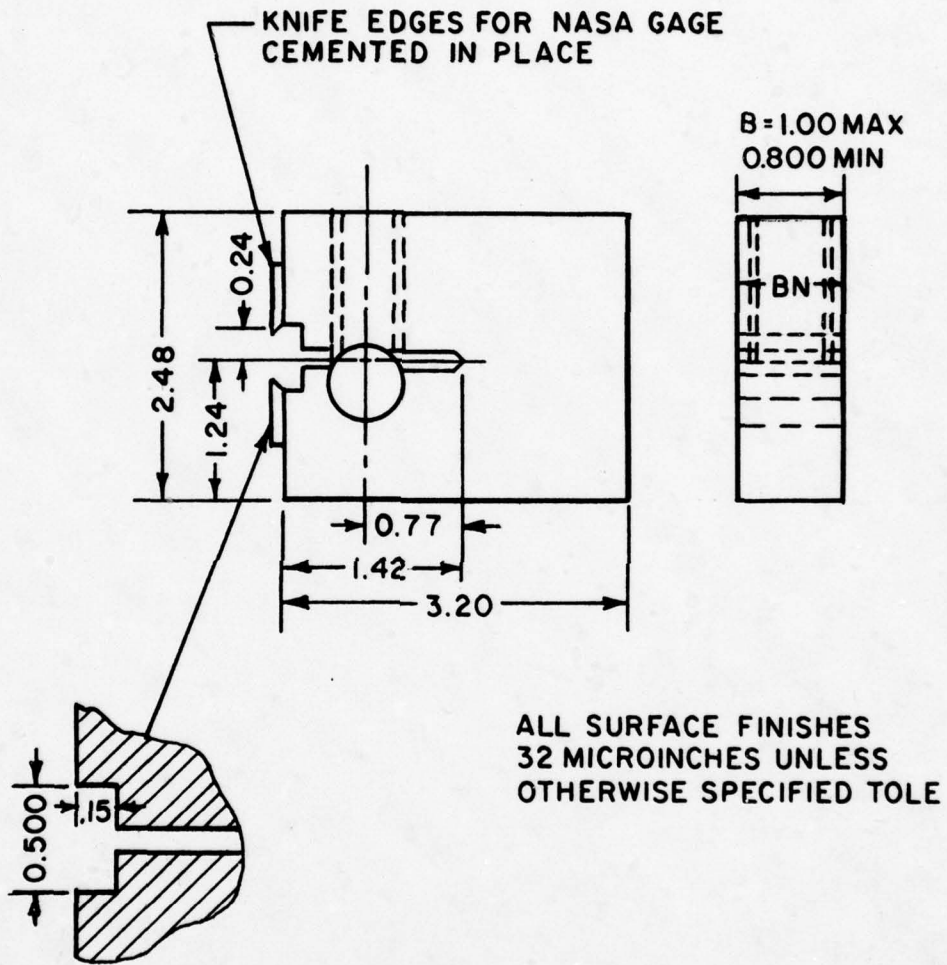
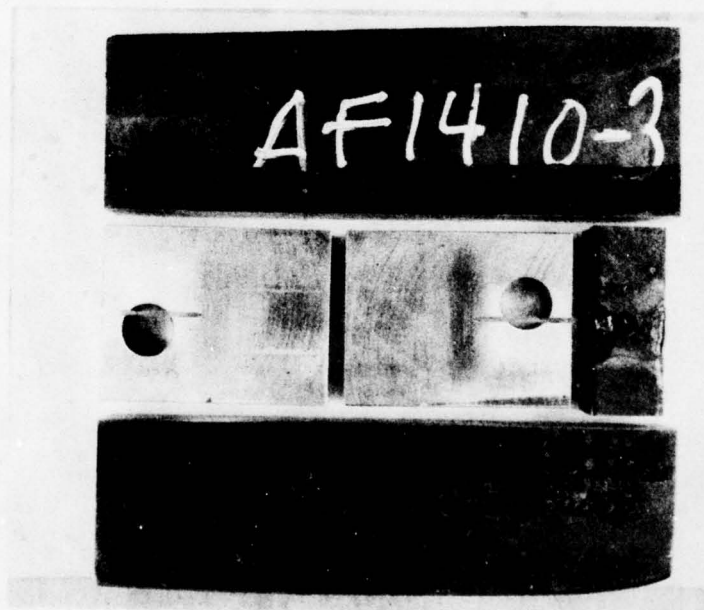


Figure 5. Detailed Drawing of Modified WOL Specimen



(a)



(b)

Figure 6 (a) - WOL Samples from Weld and Base Plate - AF-1410-2  
(b) - WOL Sample from Weld - AF-1410-3

C4708-01

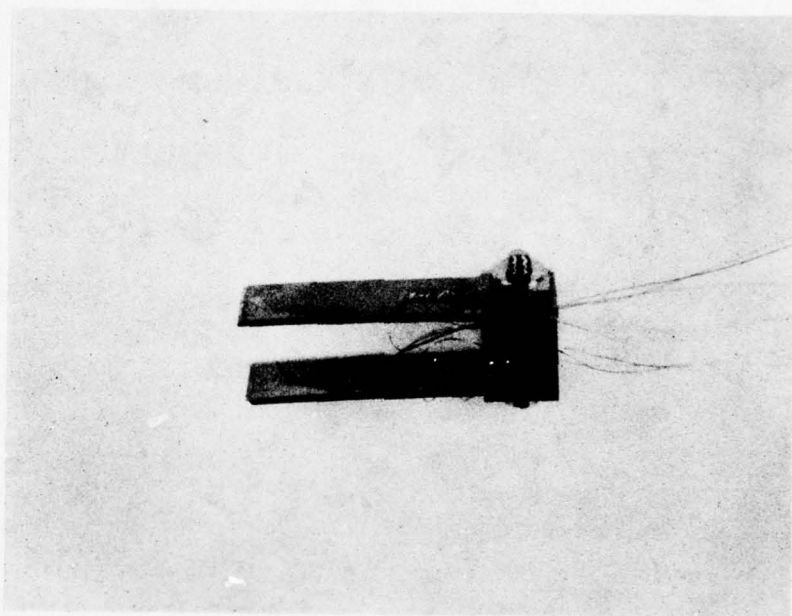


Figure 7. NASA Clip Gage with Strain Gages in Place

3-21

PRECEDING PAGE BLANK-NOT FILMED

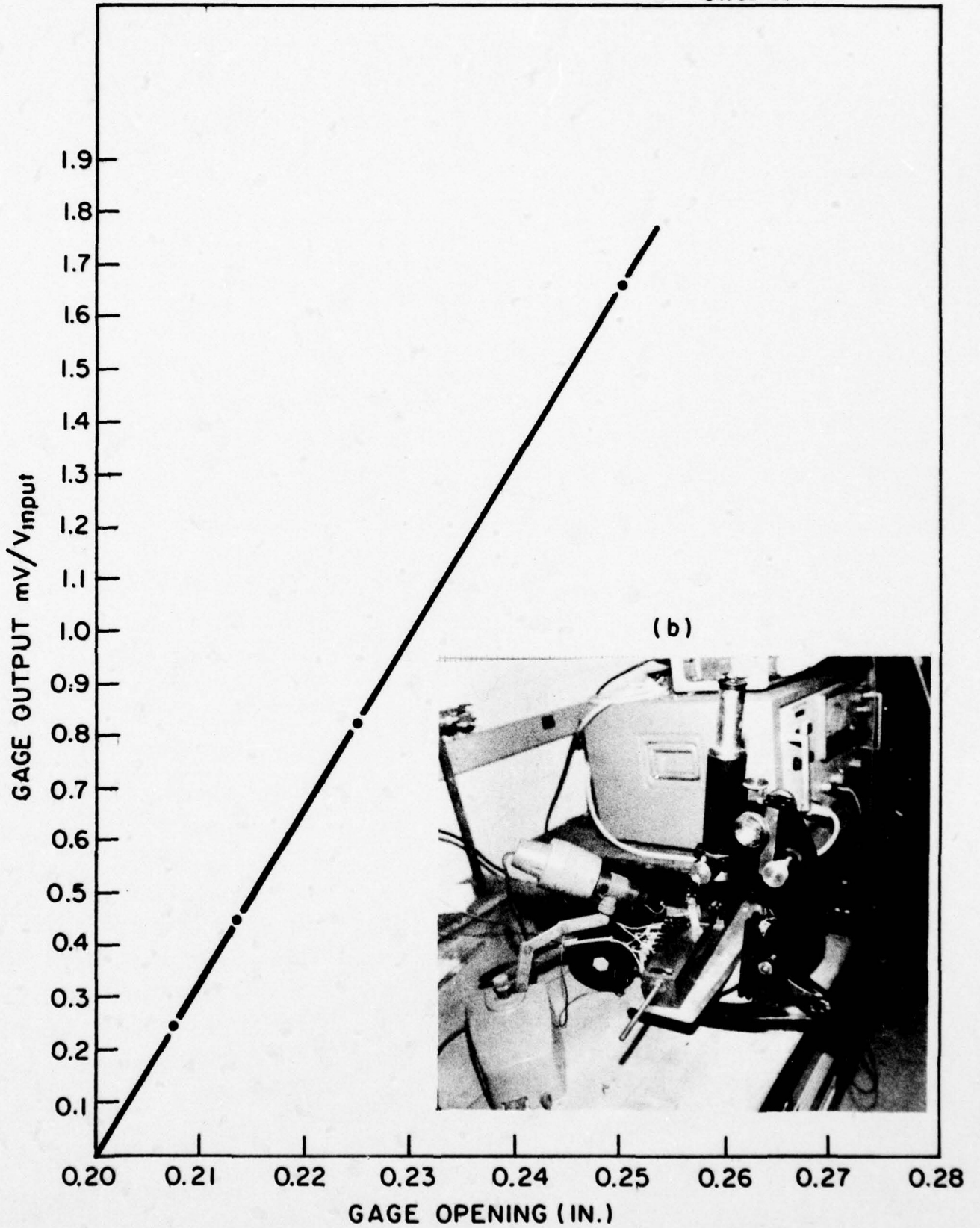


Figure 8 (a). Calibration of Gage Opening vs. Gage Output

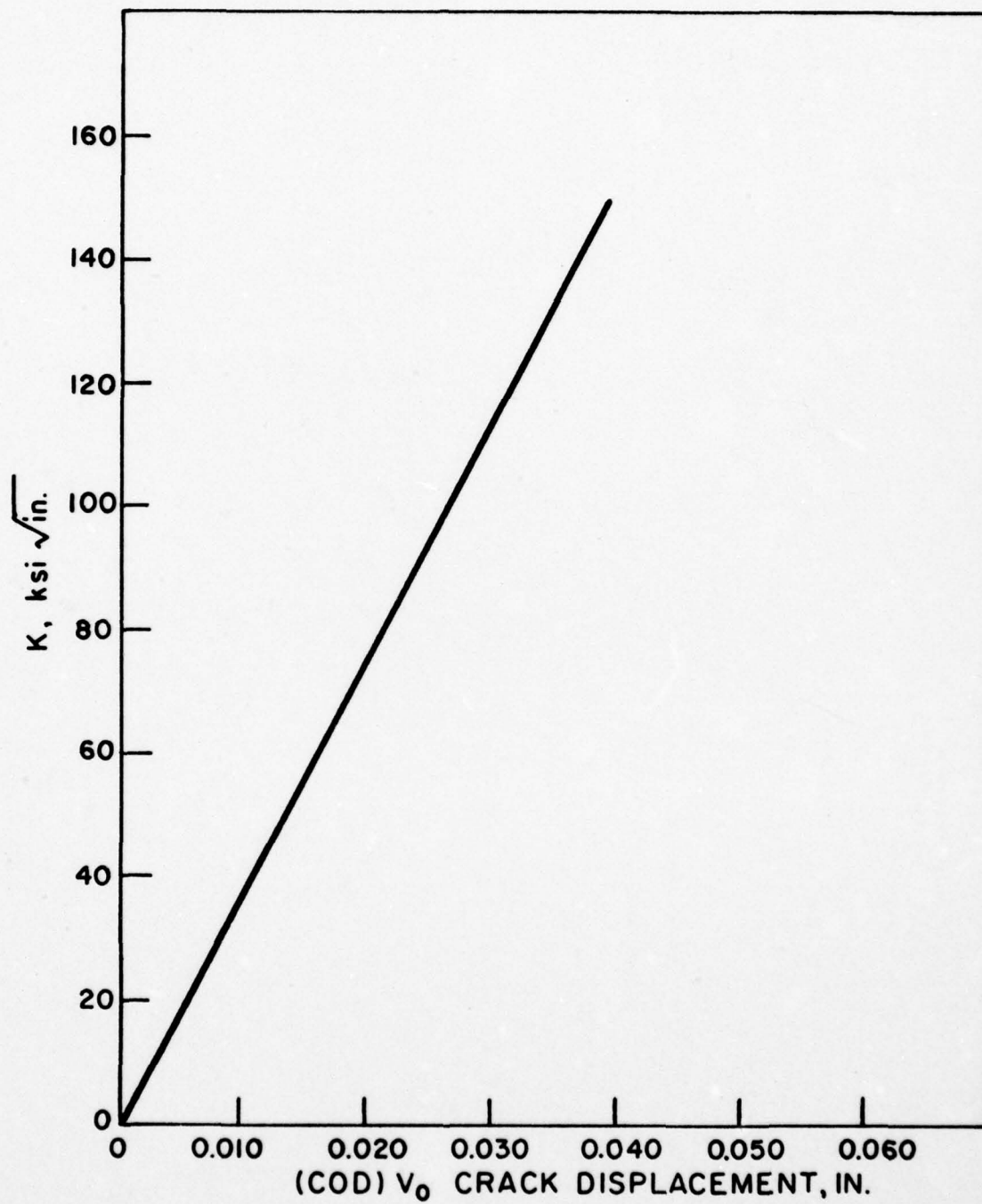


Figure 9. Correlation of  $K_1$  to  $V_0$

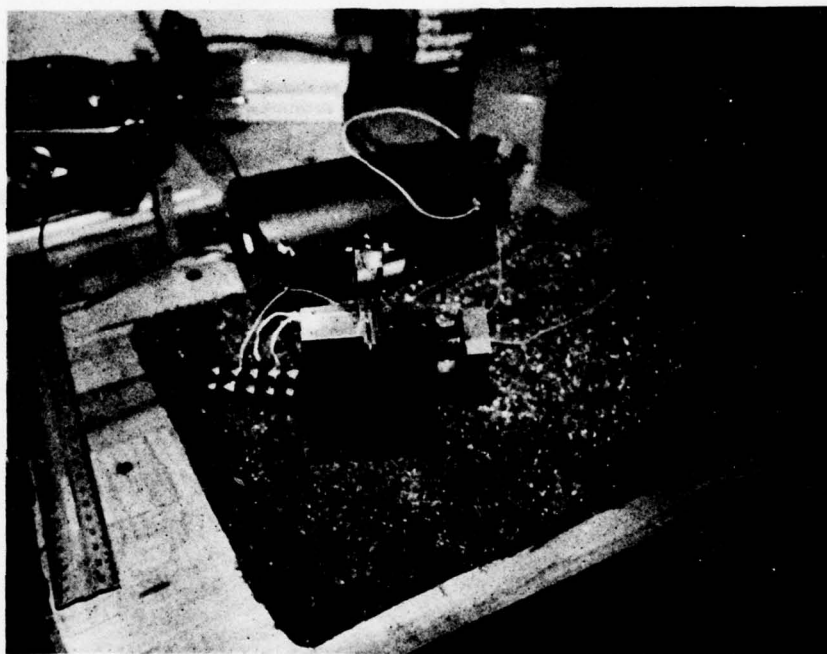


Figure 10. NASA Clip Gage Arranged on WOL Specimen  
Ready for Application of Load by Torquing Bolt

C4708-01

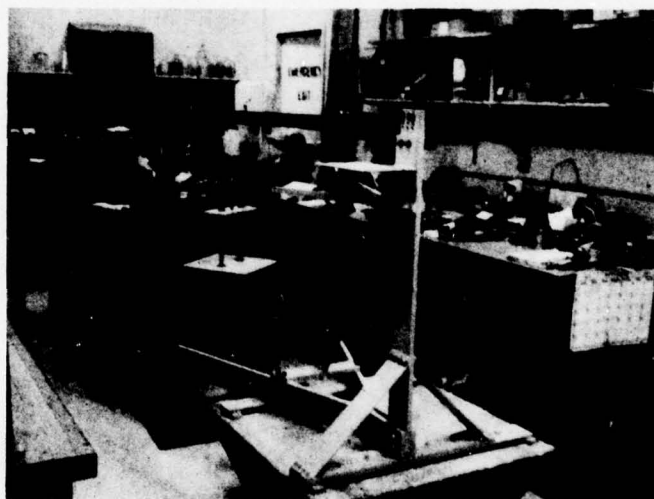


Figure 11. Cantilever Beam Test Ring for SCC Testing

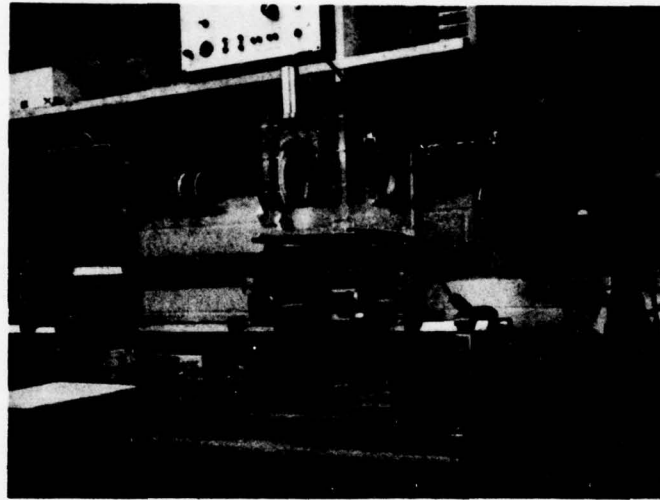


Figure 12. Cinematographic Apparatus Showing Dual 16mm Cameras - WOL Specimen and Corrosion Cell for the Continuous Monitoring of Crack Propagation

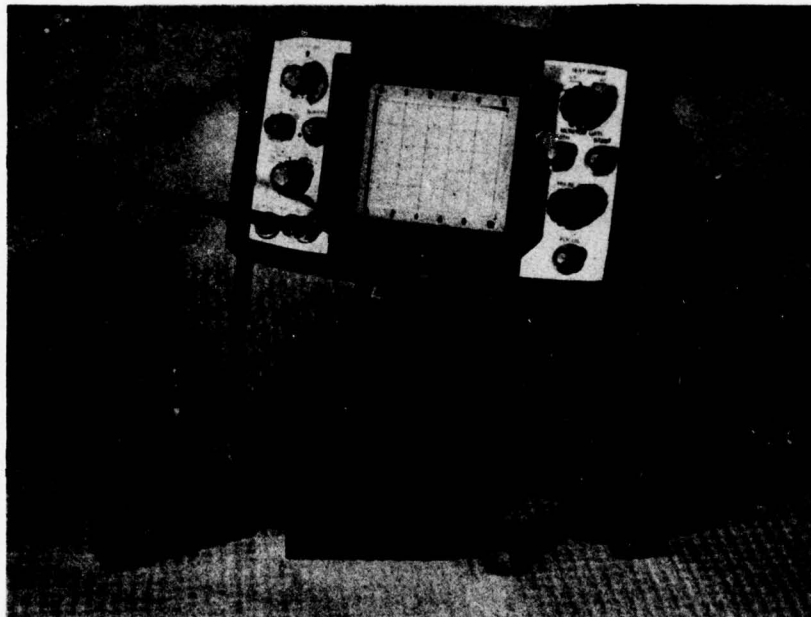


Figure 13. WOL Specimens with Transducer for Ultrasonic Evaluation of Crack Growth and the Krautkraner System

## 4. DISCUSSION AND RESULTS

### 4.1 RADIOGRAPHIC TESTS

The four test plates designated AF-1410-1, AF-1410-2, AF-1410-3 and AF 1410-4 were evaluated for soundness by Magnaflux Corporation according to the ASME Code. Their reports are given in Appendix II.

Samples AF-140-1 and AF-1410-3 contained minor porosity well within acceptable limits of the ASME code.

Sample AF-1410-2 contain a small oxide inclusion at the center of the weld which was easily avoided in the machining of the test samples.

Sample AF-1410-4 also contained minor porosity but within acceptable limits of the ASME code.

### 4.2 MECHANICAL PROPERTIES

The mechanical properties obtained in the fusion zone of the welds of the four test plates are given in Table IV. The results obtained by General Dynamics and reported in AFML-TR-75-148 are also tabulated for comparison.

Samples AF-1410-1, AF-1410-2 and AF-1410-3 prepared with weld wire from sheet stock exhibited tensile properties only slightly lower than those obtained in the AFML program. These properties were felt to be sufficiently close to the optimum base plate properties, however, to justify further stress corrosion cracking evaluation of these samples.

Sample AF-1410-4 prepared with 0.062" dia. weld wire described in Section 3-2 exhibited mechanical properties similar to those reported in AFML-TR-75-148 for as deposited welds (Item 3 in Table IV). These results are encouraging since they demonstrate the feasibility of utilizing weld wire of the same composition as the base plate to achieve mechanical properties comparative to the base plate. These results also enable us

to proceed with further studies proposed for the next period of the grant since a supply of controlled base plate and weld wire will be readily available.

Table IV. Mechanical Properties of Welds

Plate Condition Prior To Welding	Post Weld Treatment	Ultimate Tensile Strength	Yield Strength .2% Offset	Elongation	% Red. in Area	Charpy V-notch Ft-lbs.
1. Aust/WQ	As-depos.	235.9	206.4	-	65.7	-
2. Aust/WQ	950°F-4hrs	233.3	223.3	14	62.5	36 to 50
3. 950°F-4hrs	As Depos.	234.6	209.6		38.5	45 to 61
AF-1410-1	As Depos.	224	190.0	14	47.5	56 to 64
AF-1410-2	As Depos.	212.5	200	16.5	64.0	78
AF-1410-3	As Depos.	230.0	207.5	20.5	65	100
AF-1410-4	As Depos.	241.9	205.4	21.0	66.6	55 to 65

Comparison of Mechanical Properties 1, 2 and 3 from AFML-TR-75-148, Technical Report to AF-1410 plates welding in present program.

#### 4.3 WOL SCC TESTS IN 3.5% NaCl

WOL specimens were machined and fatigue cracked by MetCut Research Associates from AF-1410-2 and AF-1410-3. The notch and fatigue cracks were oriented parallel to the weld. Figure 6(a) and (b) shows the two WOL samples machined from the 8" x 8" welded plate. The small remaining section was used for the evaluation of mechanical properties.

Since MetCut Research is presently involved in an SCC evaluation program of Universal Cyclops AF-1410 base plate, it was felt that one of the WOL weld samples should be tested by that laboratory to establish a comparison with FIRL tests. AF-1410-2 plate yielded two WOL specimens of the weld and one WOL specimen of the base plate.

The initial WOL samples at both laboratories were loaded to  $K_{10}$  of 40 ksi  $\sqrt{\text{in}}$  as described in Section 3.3.1 and exposed to a 3.5% NaCl solution for periods extending to beyond 1000 hrs.

MetCut Research reported crack propagation in the weld samples after approximately 2200 hrs. The fracture surface of this sample is shown in Figure 14(a).

Two non-connected crack fronts were found to be present. Apparently two separate fatigue cracks were nucleated at the notch which did not join as the cracks extended into the weld metal. This central region of the specimen which corresponds to the first weld passes to be laid down resisted the nucleation and propagation of the fatigue crack. Since only the lateral surface cracks were being monitored the interior nature of the crack was not known at the time of testing.

Samples from AF-1410-2 weld tested at FIRL showed no evidence of crack propagation in the weld after approximately 1200 hrs. in test. See Figure 14(a) and (b). The development of the irregular crack tip on side 1 after 48 hours was apparently surface related. After developing, it showed no evidence of movement throughout the test. The fracture surface of this sample shown in Figure 14(b) was similar to the sample in Figure 14(a) tested by MetCut Associates. Two separate fatigue cracks also present in the sample were joined only by a small crack between them. See Figure 14(d). The fact that the fatigue crack did not propagate in the central region of the sample suggests that the central portion of the weld was of higher fatigue strength than the upper and lower portions of the weld. Nonhomogeneity in the structure of the weld appears to be the primary cause of the observed differences in fatigue strength. The central region of the weld corresponding to the region of the joint which experienced a maximum number of thermal reversals exhibited an extremely fine martensitic structure seen in Figure 18. The deposited fusion zone microstructure seen at the top of the weld, Figure 17, was coarse grained with coarse lath martensite. The crack shape present in both the MetCut and the FIRL tested samples precludes any meaningful estimate of  $K_{ISCC}$  for the AF-1410-2 weld fusion zone.

A WOL sample from the base plate in the double austenitized and aged (940 °F - 5 hrs.) condition was also tested at  $K_{10} = 40$  ksi in 3.5 NaCl solution. Crack growth was monitored over a period of time extending to approximately 1500 hrs.

What appeared to be crack branching occurred early in the test after 48 hrs. on side 2 and after 400 hrs. on side 1 as shown in Figure 15. The double crack continued to propagate through the entire test.

After the test, the sample was fractured to reveal the fatigue and SCC crack front as seen in Figure 14(c). The fatigue crack in this case was continuous across the specimen and the extension of the SCC crack was clearly visible as seen in Figure 14(e). No evidence of crack branching was found on the fracture surface however. The branching effect observed was apparently associated only with the surface layers. The primary crack branched as it exited at the surface.

$K_{ISCC}$  for the base plate calculated on the basis of the final crack length measurement on the fracture surface was 32 ksi  $\sqrt{\text{in.}}$

Crack growth extension vs. time data are plotted in Figure 16 for sides #1 and #2 of AF-1410 base plate. One finds a lagging of the crack on side 1 due primarily to a longer incubation time. The process as seen on both sides of the specimen consisted of an initial rapid growth stage, a second slow crack growth stage and finally crack arrest. The rates of crack growth estimated from the slope of the curves plotted in Figure 16, for stage 1 was about 0.002"/hr. and for stage 2 about 0.0002"/hr.

Crack growth rates will be determined for the welds and compared to the base plate in the next period of this program. It is anticipated that crack growth rates will be affected by nonhomogeneities arising in the fusion zone.

Recent values of  $K_{ISCC}$  for AF-1410 in the double austenitized and aged condition reported by Rockwell International in Report AFFDL-TR-77-73 were also of the order of 30 ksi  $\sqrt{\text{in.}}$  while values for the fusion zone of welded AF-1410 were the order of 60 to 70 ksi  $\sqrt{\text{in.}}$

Before any meaningful  $K_{ISCC}$  values can be obtained for the weld zone however, a greater amount of microstructural homogeneity of the weld must be obtained which will enable the development of continuous fatigue cracks across the specimen thickness.

Sample AF-1410-3 appears to have greater microstructural homogeneity than AF-1410-2 as evidenced by the microstructures seen in Figure 21. The relationship of microstructural inhomogeneities to the development of a straight fatigue crack front will be examined in more detail in the next 12 month period.

Preliminary tests will establish limits for loading of the specimen for in situ cinematographic studies. The two WOL samples notched and fatigue cracked at the fusion zone from AF-1410-3 are ready for test. One sample will be periodically removed from the 3.5% NaCl solution and SCC crack propagation will be documented. The second WOL sample will be placed in the corrosion cell shown in Figure 12 and SCC crack propagation will be continuously monitored through a low power microscope and recorded on 16mm Ektachrome film. Time lapse photography of crack motion will yield both crack rate and crack path data.

The utilization of ultrasonics to monitor crack growth at the center of the specimen has not presently been evaluated fully. Further investigation of its application to these in situ studies is anticipated in the next 12 month period.

#### 4.4 METALLURGICAL AND CHEMICAL HOMOGENEITY OF WELDS

The fusion zone of weld cross sections are seen in Figure 17(a) and (b) were studied with the SEM for both metallurgical and chemical homogeneity. The compositional and hardness variations observed on the cross sections from top to bottom of the fusion zones are given in Tables V, VI and VII. The region designated top of weld represents the final passes of the weld. The compositional variation of Cr, Mn, Fe, Co, Ni, and Mo through the weld zone of plates AF-1410-2 and AF-1410-3 was minimal. Variations in the Mo content for AF-1410-4 were greater than observed for

the two prior welds. It is not certain whether this variation is significant at this point due to the large error usually associated with determination of low element levels by SEM microprobe methods.

Back scattered electron SEM micrographs taken at the locations shown in Table V and VI are shown in Figures 18, 19 and 20, and Figures 21, 22, 23 respectively. SEM studies at the locations shown in Table VII were not completed during this period. Characterization of welds made with the 0.062" dia. wire will be conducted during the next 12 month period.

Sample AF-1410-2 exhibited lower strength than AF-1410-3 as shown in Table IV. The microstructure of AF-1410-2 weld consisted of a coarser lath martensite with more micro porosity than the AF-1410-3 weld. The coarser lath martensite and larger grain size for AF-1410-2 was apparent in Figures 17 to 20 when compared to Figures 20 to 22. Microporosity is also apparent in Figure 18 for AF-1410-2.

These microstructural differences may account for the differences in mechanical properties as suggested by Little and Machmeier. The effect of weld bead size and average cell diameter on the mechanical properties is shown in Figure 26. For an average cell diameter of  $20 \times 10^{-3}$  estimated from Figure 20 at position 1 a value of UTS of 237 ksi and T.Y. of 210 ksi and CVN = 43 ft. lbs. for the as deposited fusion zone is predicted. The values obtained and shown in Table IV agree closely with the predicted values with the exception of the CVN value of 100 ft. lbs.

The fusion zone mechanical properties are also strongly dependent upon the bead size parameter. The yield strength and notch toughness increase and decrease respectively with increase in the bead size parameter. The advantage of a small bead size was demonstrated in the optimization of the mechanical properties.

The effect of these parameters on the stress corrosion cracking susceptibility of AF-1410 has not been reported but will be investigated in the next period of this program.

#### 4.5 CANTILEVER BEAM SCC TESTS

Cantilever beam tests have not been started in this period of the program although comparative WOL and Cantilever beam SCC tests of welded samples are anticipated in the next 12 month period of the program.

Cantilever beam tests yield more well defined end points in the estimation of  $K_{ISCC}$  and will allow samples to be tested both parallel and perpendicular to the weld bead. However, crack propagation studies are best conducted utilizing the WOL samples.

In view of the lower values of  $K_{ISCC}$  being obtained for these samples in 3.5 NaCl solutions a recalculation for the minimum specimen size for plane strain conditions can be made based upon the criteria that

$$B \geq 2.5 \frac{K_{IC}^2}{\sigma_{ys}} \quad \text{for plane strain}$$

where B = specimen thickness

$$\text{For } K_{IC} = 90 \text{ ksi } \sqrt{\text{in}}$$

$$\text{and } \sigma_{ys} = 200 \text{ ksi}$$

$$B \geq 0.5''$$

The minimum value of 0.5 for specimen thickness satisfying plane strain conditions allow us to consider the utilization of WOL specimens 1/2 the size used for the initial studies.

The smaller samples will be more economical both from the welding and machining point of view in addition to enabling us to obtain 4 samples from each 8 x 8" plate.

TABLE V

AF-1410-2

<u>Location</u>	Hardness R <sub>C</sub>	Cr	Mn	Fe	Co	Ni	Mo
Weld 1	42.6	1.8	.01	74.5	13.4	9.8	1.5
Weld 2	44.0	1.8	.01	74.2	13.9	9.8	1.2
Weld 3	46.4	1.9	.02	74.2	14.0	9.9	1.0
Weld 4	46.4	2.0	.01	73.4	14.8	9.4	1.0
Weld 5	44	1.7	.03	73.2	14.1	9.7	1.3
Weld 6	45	1.9	.01	72.8	13.3	9.8	1.0
Base Plate 7	45.2	1.9	.01	74.0	14.1	9.9	1.0
Base Plate 8	45	2.1	.01	74.0	14.3	9.2	1.4

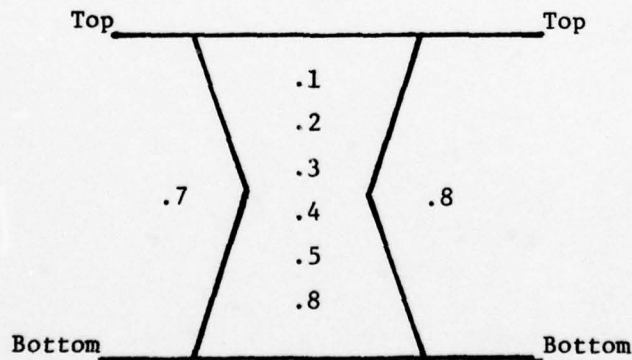


TABLE VI

AF-1410-3

Location	Hardness R <sub>C</sub>	Cr	Mn	Fe	Co	Ni	Mo
Weld 1	41.5	1.9	0.01	72.8	13.6	9.2	0.7
Weld 2	44.5	1.8	0.01	71.3	13.9	9.2	1.0
Weld 3	42.5	2.0	0.01	74.3	13.7	9.2	1.1
Weld 4	44.5	1.9	0.03	72.9	14.2	9.3	1.0
Weld 5	44.1	1.9	0.03	72.5	14.2	8.7	1.1
Weld 6	44.9	2.0	0.01	74.2	14.4	9.5	.7
Base Plate 8	45.2	2.0	0.01	72.8	14.0	9.3	1.1
Base Plate 9	45.0	1.9	0.03	73.6	14.7	9.2	1.2

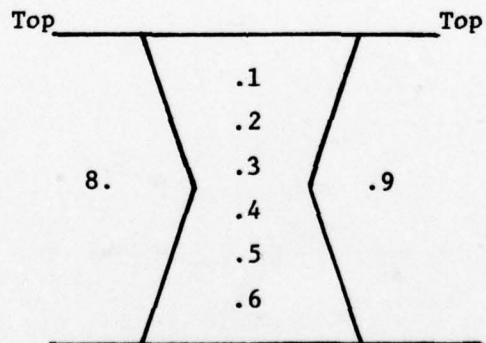
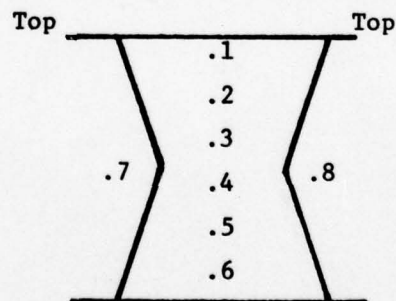
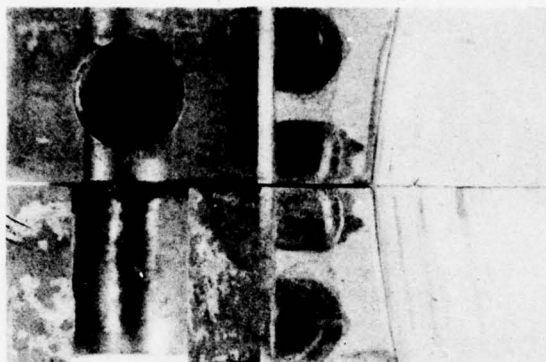


TABLE VII

AF 1410-4

Location	Hardness R <sub>C</sub>	Cr	Mn	Fe	Co	Ni	Mo
Weld 1	48	1.9	0.07	72.7	13.2	8.8	1.0
Weld 2	49.5	1.9	0.01	74.4	14.2	9.1	.8
Weld 3	48.5	2.1	0.01	74.7	13.6	9.2	.2
Weld 4	45.5	2.1	0.01	77.9	14.6	9.8	.5
Weld 5	51.0	2.0	0.01	77.4	14.2	9.0	1.5
Weld 6	49.5	1.9	0.01	77.0	14.0	9.8	1.0
Base Plate 7	47	1.9	0.01	75.0	14.2	9.8	1.4
Base Plate 8	47.5	2.1	0.01	77.1	14.1	9.6	1.2

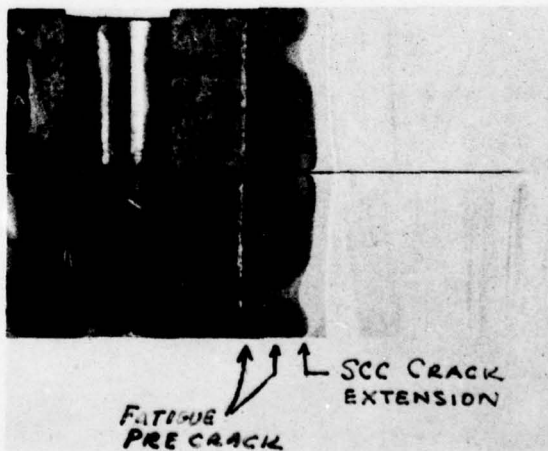




a



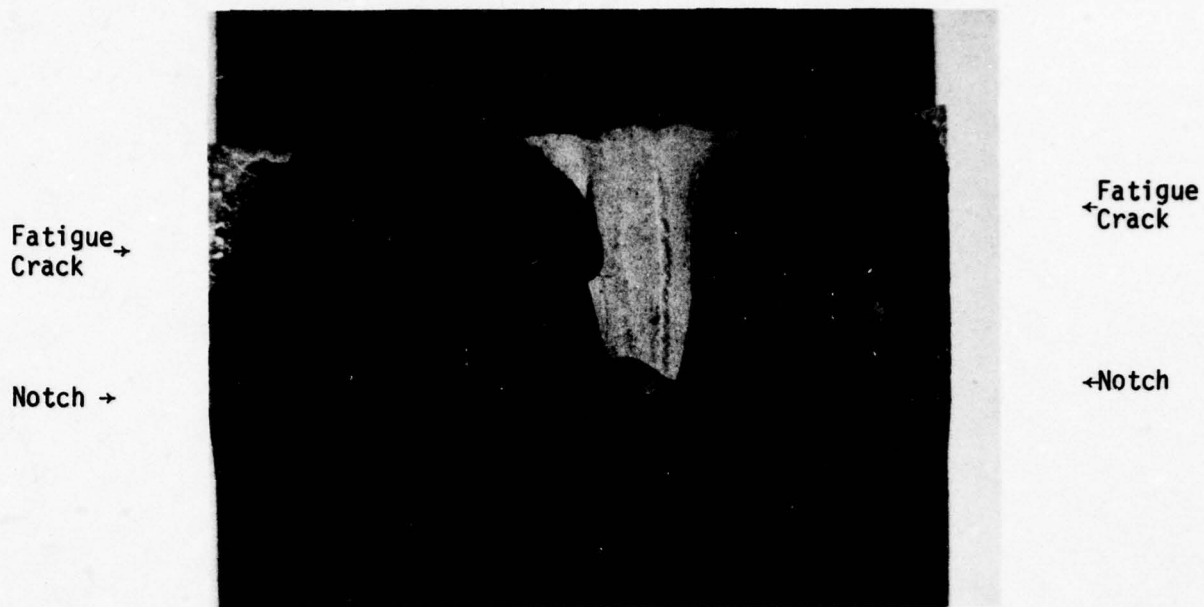
b



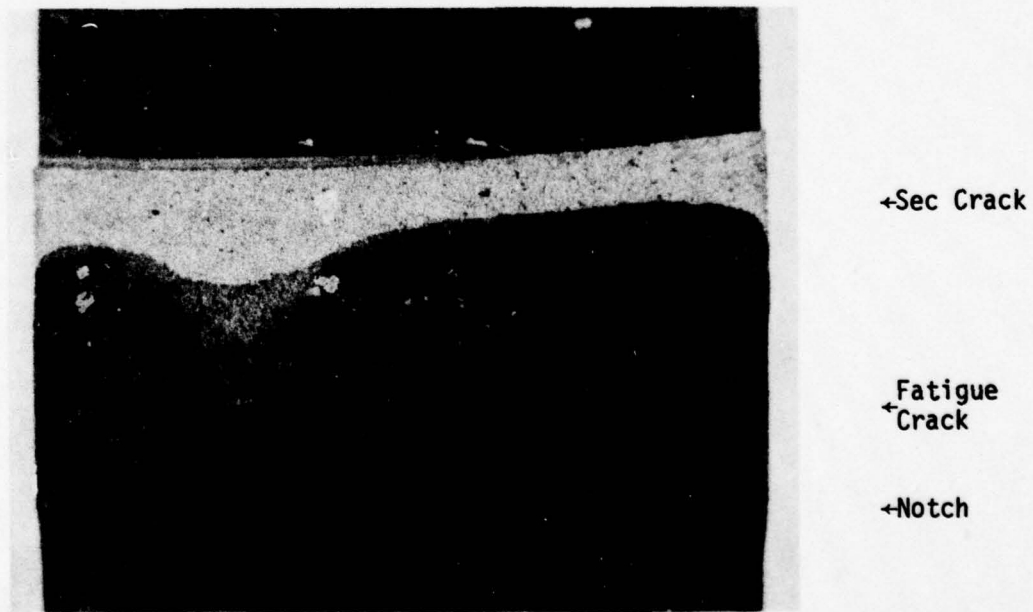
c

Figure 14 (a) Fracture Surface of AF 1410-2 Weld Tested by MetCut  
(b) Fracture Surface of AF 1410-2 Weld Tested by FIRL  
(c) Fracture Surface of AF 1410 Base Plate Tested by FIRL

PRECEDING PAGE BLANK-NOT FILMED



(d)



(e)

Figure 14 (d) Enlarged View of Figure 14(b) Showing Irregular Fatigue Crack Front  
(e) Enlarged View of Figure 14(c) Showing Fatigue Crack and Sec Crack

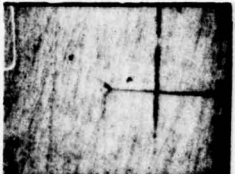
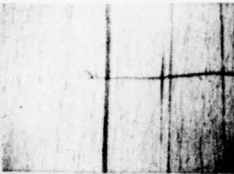

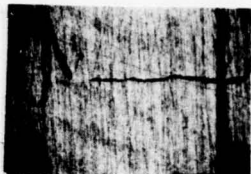
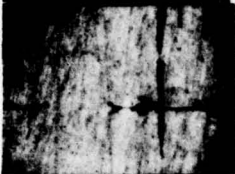
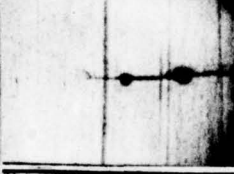
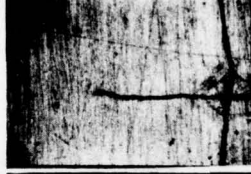









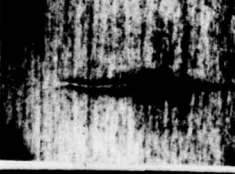



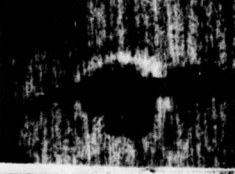





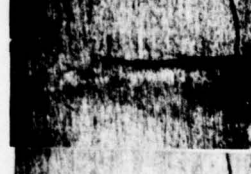
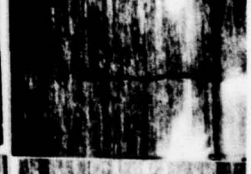

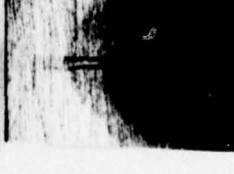


Base Plate		Hrs.	Weld		Date
Side 1	Side 2		Side 1	Side 2	
		0			2/14/78
		24			2/15/78
		48			2/16/78
		480			3/6/78
		504			3/7/78
		528			3/8/78
		648			3/13/78
		696			3/15/78

Figure 15. Crack Propagation in AF-1410-2 Weld and Base Plate

$$K_{10} = 40 \text{ ksi } \sqrt{\text{in.}}$$

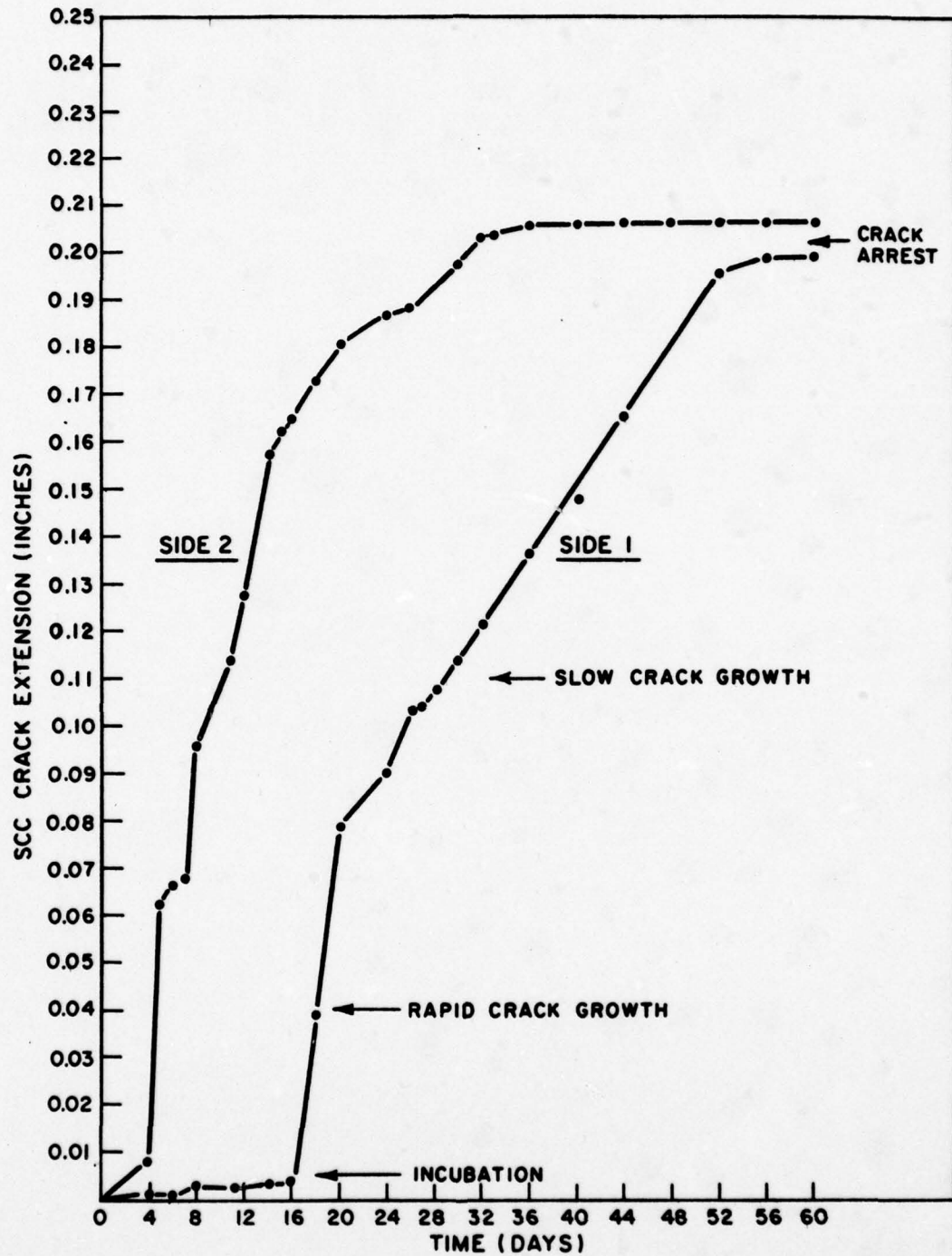


Figure 16. Crack Extension vs. Time WOL Test of AF-1410  
Base Plate  $K_{10} = 40 \text{ ksi } \sqrt{\text{in.}}$

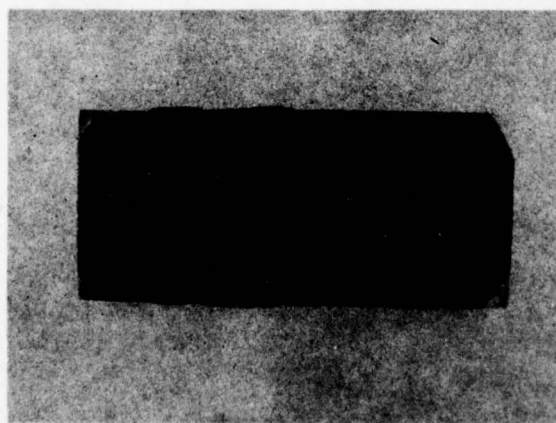
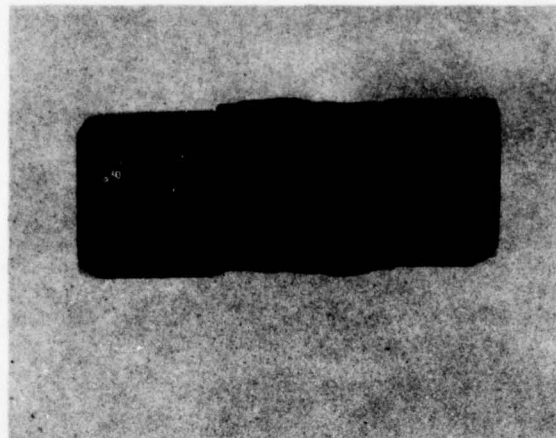
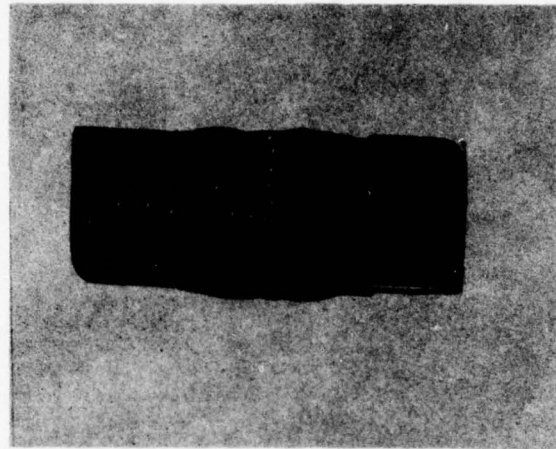
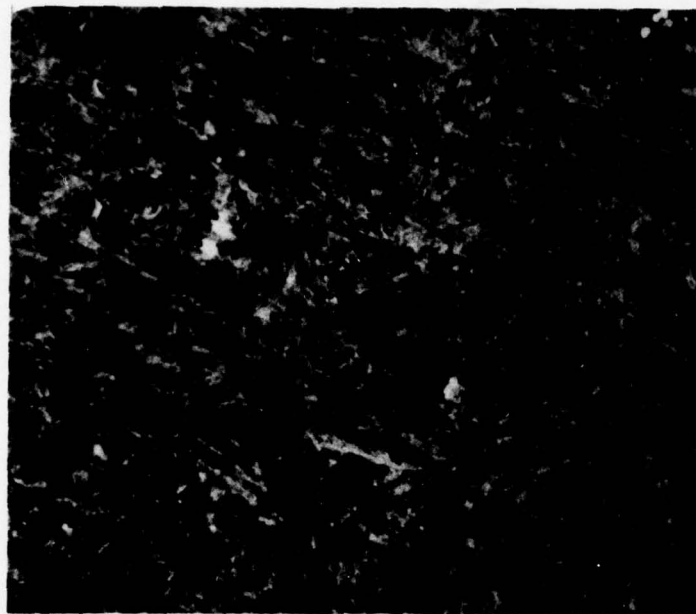


Figure 17. Weld Cross Sections with Hardness Impressions  
a) AF 1410-2  
b) AF 1410-3

C4708-01

1



2

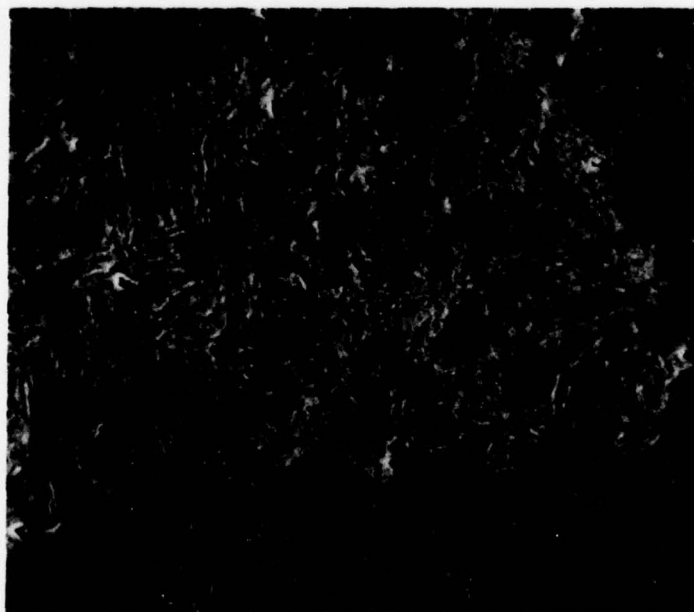


Figure 18. Back Scattered Electron Image of Weld AF-1410-2 at Positions 1 and 2 Shown in Table V. Mag. 500X

C4708-01



3

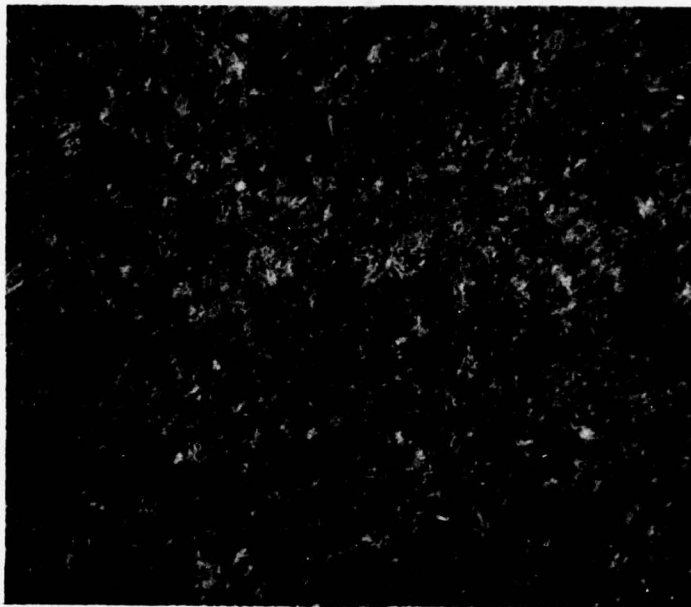


4

Figure 19. Back Scattered Electron Image of Weld AF-1410-2 at Positions 3 and 4 Shown in Table V. Mag. 500X.

C4708-01

5



8

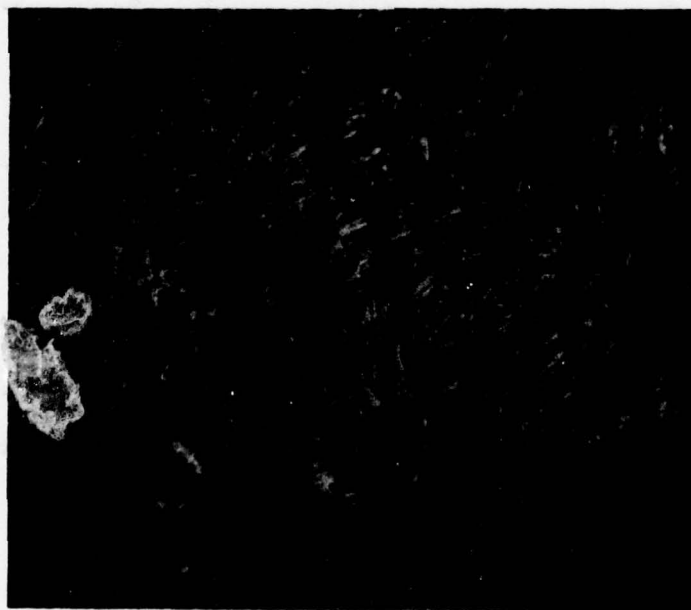


Figure 20. Back Scattered Electron Image of Weld AF-1410-2 at Positions 5 and 8 Shown in Table V. Mag. 500X.

C4708-01



1

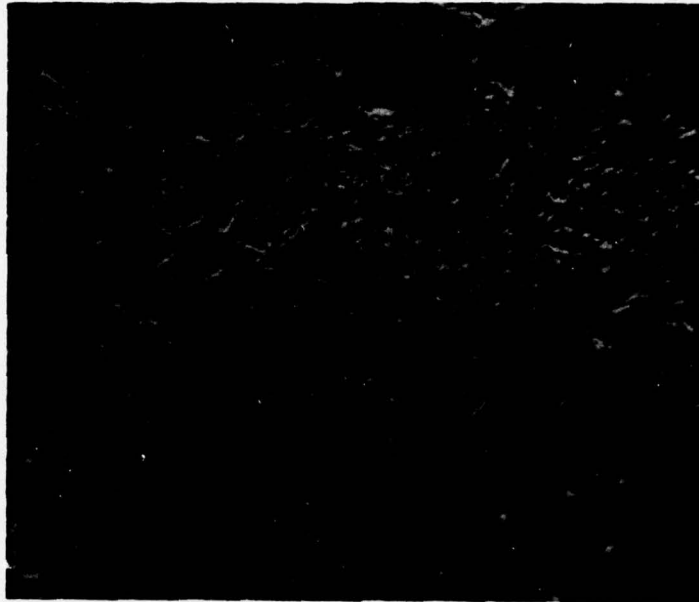


2

Figure 21. Back Scattered Electron Images of Weld AF-1410-3 at Positions 1 and 2 Shown in Table VI. Mag. 500X.

C4708-01

3



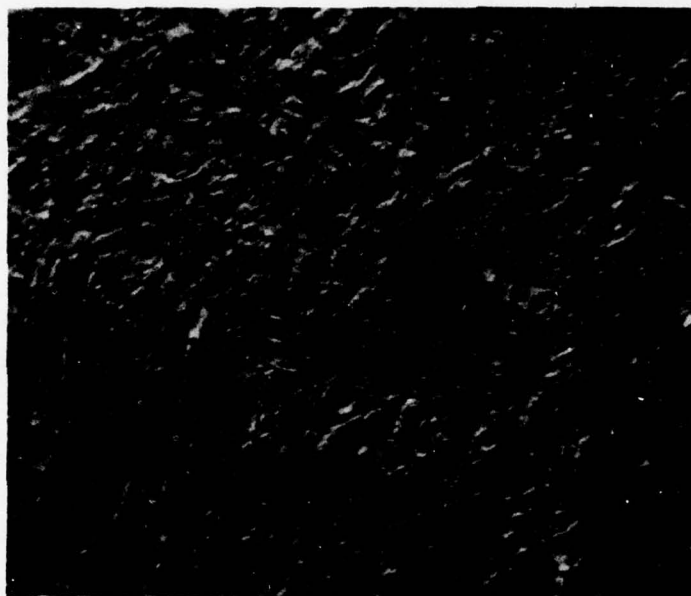
4



Figure 22. Back Scattered Electron Images of Weld AF-1410-3 at Positions 3 and 4 shown in Table VI. Mag. 500X.

C4708-01

5



6

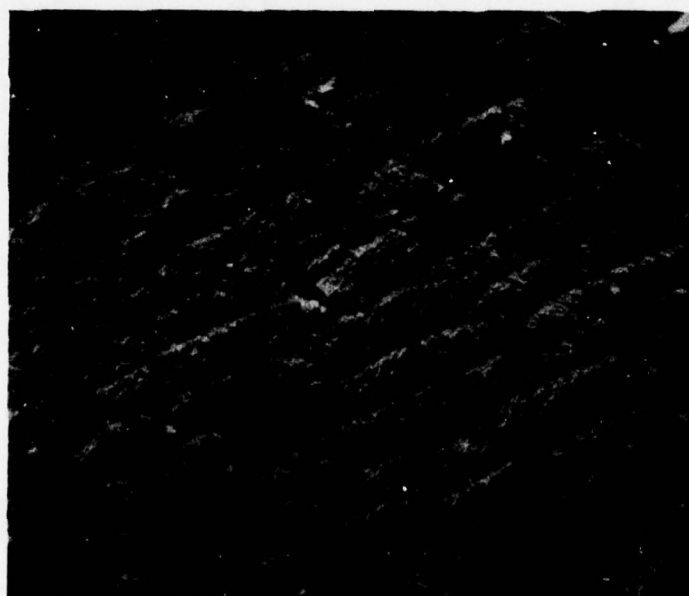


Figure 23. Back Scattered Electron Images of Weld AF-1410-3 at Positions 5 and 6 Shown in Table VI. Mag. 500X.

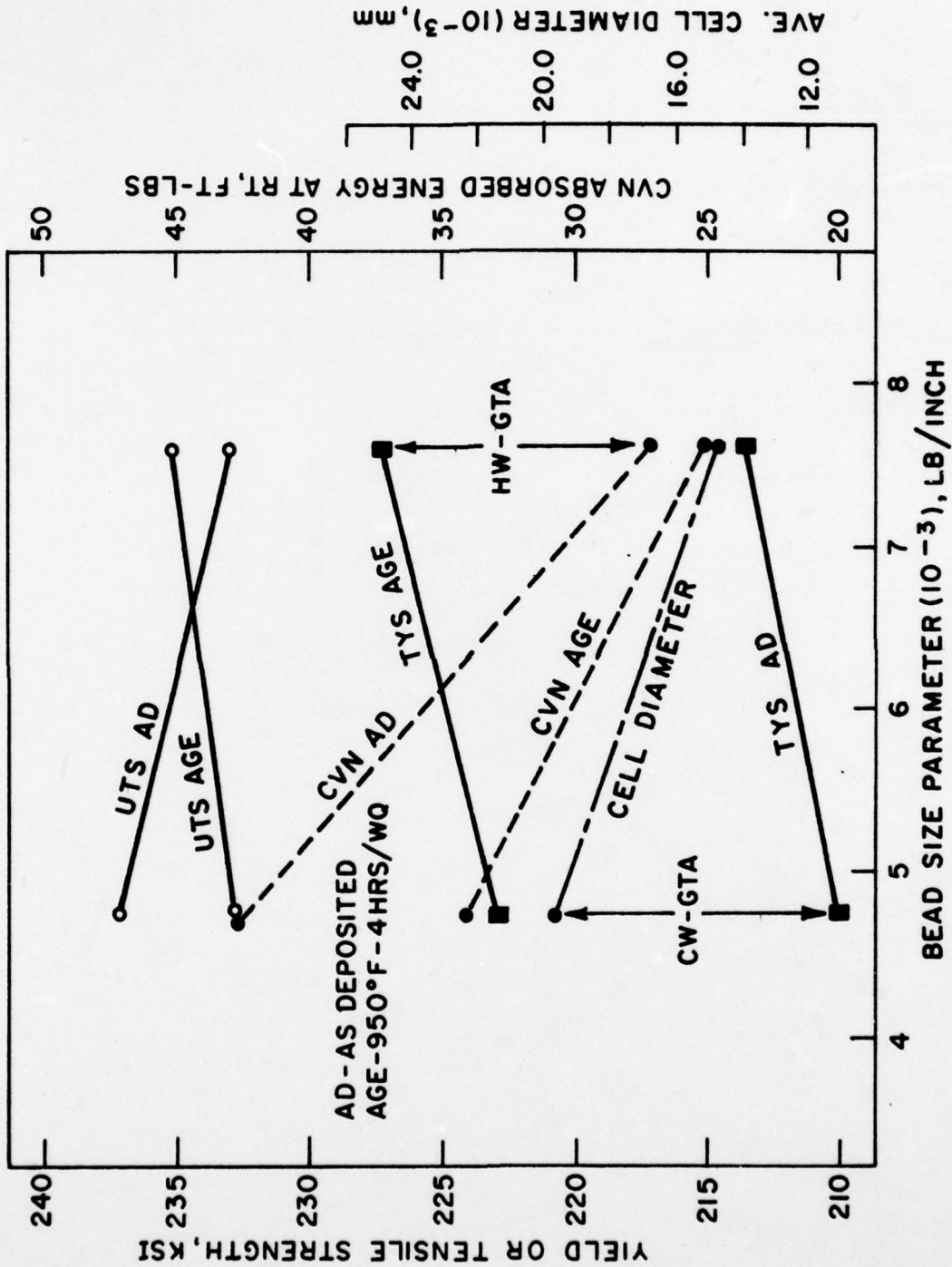


Figure 24. Fusion Zone Mechanical Properties from Little & Machmeier

## 5. FUTURE WORK

AF-1410 plates measuring 4" x 8" x 5/8" thick will be joined by means of cold wire-gas tungsten arc welding procedures outlined in this report. The weld wire will be 0.062" dia. wire prepared by Universal Cyclops having the same composition as the base plate. Samples joined along the 8" edge will provide 3 WOL specimens for SCC tests. Samples joined along the 4" edge will also provide 3 cantilever beam specimens notched perpendicular to the weld and 3 cantilever beam specimens notched perpendicular to the weld. SCC testing will be initially conducted in 3.5% NaCl solutions but will be followed by testing in dry and moist gaseous environments.

All sample machining and fatigue cracking will be conducted by MetCut Associates. SCC tests will be conducted at the Franklin Institute Research Laboratories. The welds will be characterized for mechanical properties including tensile and charpy V notch properties and for chemical and microstructural homogeneity.

Crack path and propagation rates will be monitored on the external surfaces of the sample both by interrupted testing and by in situ studies utilizing cinematography.

All samples will be fractured upon completion of the test to determine crack extension and crack front characteristics.

$K_{ISCC}$  will be estimated for both the WOL and cantilever beam tests according to ASTM recommended practices.

## 6. SUMMARY

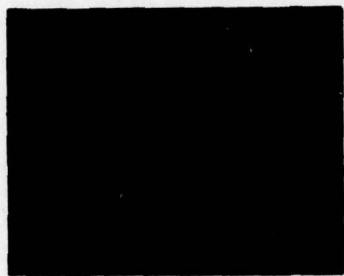
1. AF 1410 plates 5/8" and 1" thick were procured in the double austenitized condition from Universal Cyclops through AFML.
2. Filler weld rods were prepared having the same composition as the base plate by shearing sheet stock into strips 1/16" x 13".
3. Through the use of GTA cold wire manual feed, 5/8" and 1" plates were welded using the fabricated filler weld rods. These welds were sound and (charpy V notch) CVN and tensile properties were similar to the properties obtained for welds prepared by General Dynamics and reported in AFML-TR-75-148.
4. The necessary equipment and fixtures were assembled to conduct WOL and cantilever beam SCC tests - Equipment for cinematography was also acquired to study in situ crack propagation on both sides of the WOL specimen.
5. WOL specimens were prepared from two welded assemblies. Compositional and metallurgical analysis of the weld was conducted with the scanning electron microscope.
6. SCC tests were conducted on both welded samples and the base plate and crack propagation was monitored on both sides of the sample.  $K_{ISCC}$  for base plate was estimated to be 32 ksi  $\sqrt{\text{in}}$ . Weld samples did not readily propagate for loadings of  $K_{10} = 40$  ksi  $\sqrt{\text{in}}$ .
7. Fracture surface examination of the fatigue and SCC crack revealed two non-connected cracks in the welded sample reflecting nonhomogeneity in the welded microstructure. These findings precluded valid  $K_{ISCC}$  data.
8. A test plate was welded utilizing 0.062" weld wire produced by Universal Cyclops. The mechanical properties were similar to the properties obtained with the weld wire procedure from sheet. These tests demonstrate that suitable welds having mechanical properties similar to base plate properties could be prepared using weld wire of the same composition as the base plate.
9. Further indepth studies of the stress corrosion cracking susceptibility of welded AF 1410 plates is proposed for the next 12 month period in both aqueous and gaseous environments.

## REFERENCES

1. Routh, W. E., "Lower Cost by Sutstituting Steel for Titanium", AFFDL-TR-77-73, under Contract F33615-75-C-3109.
2. Novak, S.R. and Rolfe, S.T., "Modified WOL Specimen for  $K_{ISCC}$  Environmental Testing", *Journal of Materials JMLSA*, Vol. 1.
3. Fisher, D. M., Bubsey, R.T. and Srawley, J. E., "Design and Use of Displacement Gage for Crack Extension Measurements", NASA TN D-3724, NASA Research Center, Cleveland, Ohio.
4. Brown, B. T., "A New Stress Corrosion Cracking Test for High Strength Alloys", *Materials Research and Standards*, Vol. 6, No. 3, March 1966, pp. 129-133.
5. Klema, S. J., Fisher, D. M. and Buzzard, "Monitoring Crack Extension in Fracture Toughness Tests by Ultrasonics", *Journal of Testing and Evaluation*, JTEVA, Vol. 4, No. 6, Nov. 1976, pp 397-404.

ACKNOWLEDGEMENTS

This is to acknowledge the assistance of Mr. Hugh Kelly in the welding of AF 1410 plates, Mr. Louis Cinquina for his assistance in the conducting of the stress corrosion cracking tests and the setting up of the equipment, and of Richard Fiore for his contribution in the scanning electron microscopy studies.



---

**Appendix**

I

FRACTURE MECHANICS APPROACH TO SCC



**THE FRANKLIN INSTITUTE RESEARCH LABORATORIES**  
THE BENJAMIN FRANKLIN PARKWAY • PHILADELPHIA, PENNSYLVANIA 19103

## FRACTURE MECHANICS APPROACH TO SCC

The fracture mechanics approach is generally used as the most reliable method to establish the sensitivity of materials to stress corrosion cracking. The resistance of high strength steels to sea water stress corrosion cracking is characterized in terms of a threshold level of stress intensity below which SCC does not occur. The threshold level of stress intensity, defined in linear elastic fracture mechanics as  $K_{I\text{ SCC}}$ , combines the threshold and flaw size and may be compared directly to the fracture stress intensity parameter  $K_{Ic}$  determined in air under plane strain condition as established by ASTM Committee E-24.

Although no standard method of test has been adopted to determine  $K_{I\text{ SCC}}$ , two techniques have been widely used and accepted as valid methods of test.

One method developed by Brown [1] is the cantilever bend test. This method employs a pre-fatigue notched bar held horizontally and surrounded at the notch by the corrodant in a molded polyethylene container. The specimen is dead weight for periods of time extending to a minimum time of 500 hours under a fixed load.

The stress intensity factor  $K_{\alpha}$  is calculated for each condition of loading as a function of time to fracture using the following relationship

$$K_{\alpha} = \frac{4.12M (\alpha^{-3} - \alpha^3)^{1/2}}{BD^{3/2}}$$

where M is the bending moment

B is the breadth of the specimen

$$B \geq 2.5 \frac{K_{Ic}^2}{\sigma_{ys}} \quad \text{for}$$

plane strain

D is the vertical depth of the specimen

$\alpha$  is defined as  $1 - \frac{a}{D}$  where a is the total initial depth of the notch plus fatigue cracking.

$K_{I\text{ SCC}}$  is defined as the value of  $K_{I\alpha}$  below which the specimen does not fail after an extended time in excess of 500 hours. Six specimens are generally required to evaluate one value of  $K_{I\text{ SCC}}$ .

A second method, developed by Novak and Rolfe [2] utilizes a modified wedge opening loading (WOL) specimen. In contrast to the cantilever bend test, the modified (WOL) test is a constant displacement test which utilizes a single precracked specimen. This latter method eliminates the need for a special fixture and facilitates the simultaneous testing of numerous specimens.

The applied  $K_I$  value at the tip of the crack is calculated using the following equation.

$$K_I = \frac{PC_3 \left(\frac{a}{w}\right)}{B(a)^{1/2}}$$

Where P = load

a = crack length

w = specimen width

B = specimen thickness

$C_3 \left(\frac{a}{w}\right)$   $C_3$  function of  $\left(\frac{a}{w}\right)$ ,

is given by

$$C_3 \left(\frac{a}{w}\right) = \left[ 30.96 \left(\frac{a}{w}\right) - 195.8 \left(\frac{a}{w}\right)^2 + 730.6 \left(\frac{a}{w}\right)^3 - 1186.3 \left(\frac{a}{w}\right)^4 + 754.6 \left(\frac{a}{w}\right)^5 \right]$$

The WOL specimen is shown in Figure 5. The crack opening is fixed by the bolt, and the loading is by constant displacement measured by means of a NASA type clip gage [3].

The cantilever beam method measures the crack extension threshold  $K_{I\ SCC}$  whereas the (WOL) method measures the arrest value  $K_{I\ SCC}$ . The crack initiation and propagation aspects can be best followed with the modified (WOL) specimen since the test can be periodically interrupted for microscopic examination without unloading the specimen. The final crack length is measured on the lateral faces of the specimen. The three dimensional aspects of the crack is determined by fracture of the sample and examination of the fracture surface. The effective crack length is determined by the relationship

$$a = \frac{a_L + a_m + a_R}{6}$$

Where  $a_m$  is the crack length at the middle of the specimen  $a_L$  and  $a_R$  are the crack lengths measured on the fracture surface on the left and right sides of the specimen respectively.

To determine changes in  $K_I$  with time as the crack propagates the crack length or can be measured periodically with a microscope and the force  $P$  and the stress intensity  $K_I$  may be calculated for any crack length  $a$  using the relationship

$$K_I = \frac{P C_3 \frac{a}{w}}{(B B_N)^{1/2} a^{1/2}}$$

where  $B$  and  $B_N$  where  $B = 1$  for a 1T specimen and  $B_N$  is the actual value of the specimen thickness.

P(load is calculated from the equates

$$P = \frac{EB V_0}{C_6 \left(\frac{a}{w}\right)}$$

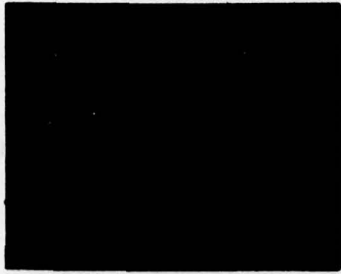
where E is the modulus

B is specimen width

$V_0$  is the initial crack opening displacement

$C_6$  if a function of  $\left(\frac{a}{w}\right)$  obtain from compliance calibration data  
and give by

$$C_6 \left(\frac{a}{w}\right) = e \left[ 3.453 - 8.097 \left(\frac{a}{w}\right) + 42.314 \left(\frac{a}{w}\right)^2 - 64.677 \left(\frac{a}{w}\right)^3 + 36.845 \left(\frac{a}{w}\right)^4 \right]$$



---

**Appendix**

II

RADIOGRAPHIC REPORTS ASME CQDE



**THE FRANKLIN INSTITUTE RESEARCH LABORATORIES**  
THE BENJAMIN FRANKLIN PARKWAY • PHILADELPHIA, PENNSYLVANIA 19103





